Thyroid Hormone Receptor Regulation of Cholesterol and Lipid Metabolism

---

A Dissertation Presented to

the Faculty of the Department of Biology & Biochemistry

University of Houston

In Partial Fulfillment

of the Requirements for the Degree

Doctor of Philosophy

By

Jean Z Lin

May 2014

Thyroid Hormone Receptor Regulation of Cholesterol and Lipid Metabolism

Jean Lin

Dr. Jan-Åke Gustafsson, Chairman

Dr. Paul Webb

Dr. David Moore

Dr. Cecilia Williams

Dr. Chin-Yo Lin

Dean, College of Natural Sciences and Mathematics

ACKNOWLEDGEMENTS

I would like to recognize my former mentor, the forefather of this research, John D Baxter. I started my research career working in his lab as a technician at UCSF and his encouragement gave me my start in scientific research.

I especially thank Kevin Phillips for the opportunity to do research in his lab. He's been the pioneer behind the research. His constant motivation has pushed me to overcome obstacles and strive to do great science and become a good scientist.

I would like to acknowledge my advisor Jan-Åke Gustafsson, and my committee members: David Moore, Paul Webb, Cecilia Williams, and Chin-Yo Lin. Their numerous suggestions and comments were immensely beneficial in my research.

I need to thanks my parents for their never-ending love; I couldn't have done this without them. They have been my pillars of support for all of life's challenges.

Additionally I would like to thank friends, classmates, and former and present lab members. Their comradeship gave me encouragement to make it through difficult periods.

Thyroid Hormone Receptor Regulation of Cholesterol and Lipid Metabolism

---

An Abstract of a Dissertation Presented to

the Faculty of the Department of Biology & Biochemistry

University of Houston

In Partial Fulfillment

of the Requirements for the Degree

Doctor of Philosophy

By

Jean Z Lin

May 2014

ABSTRACT

Thyroid hormone receptor (TR) activation affects numerous metabolic processes involved in lipid and glucose metabolism, with implications for diseases such as obesity, diabetes, and hyperlipidemia. Thyroid hormone and synthetic TR agonists are known to decrease serum lipids and induce fat loss. Here we investigate the effects of TR agonists on lipid homeostasis in the liver and adipose tissue.

TR agonists lower serum cholesterol levels in rodents, monkeys, and humans. While it is clear that TR activation reduces serum cholesterol, the mechanism behind this effect is less apparent. Although TR agonists have been reported to affect several pathways involved in cholesterol metabolism, the most notable rationale has been that thyroid hormones stimulate expression of the LDL receptor (LDLR). Here we show TR activation can markedly reduce serum cholesterol in mice devoid of LDLR by inducing Cyp7a1 expression and stimulating the conversion and excretion of cholesterol as bile acids. Thus, TR agonists may represent a promising therapeutic to treat hypercholesterolemia disorders for which LDLR induction is not fully effective.

Thyroid hormones have long been known to stimulate basal metabolic rate and elicit thermogenesis, effects generally attributed to the activation of brown adipose tissue (BAT). However, the relationship between TR activation and

thermogenesis is complex and not fully resolved. Here we show that thyroid hormone and the TR agonist GC-1 induce a BAT-like program of adaptive thermogenesis and uncoupled respiration in subcutaneous white adipose tissue (WAT), which appears to directly mediate an increase in metabolism and marked fat loss. The TR mediated conversion of white to beige fat, an action accompanied by striking anti-diabetic and anti-obesity properties, may represent an unrecognized component of TR-mediated thermogenesis and demonstrates the profound pharmacological potential of beiging of WAT.

In conclusion, we have shown that TR activation in the liver reduces serum cholesterol independent of the LDLR via the induction of hepatic Cyp7a1 and that TR activation in WAT elicits a functional conversion of white to brown fat. *These data show the TR activation has beneficial effects on lipid homeostasis in the liver and adipose tissue and may suggest an important strategy to combat metabolic diseases.*

TABLE OF CONTENTS

CHAPTER 1 INTRODUCTION 1

THYROID HORMONE: MECHANISM OF ACTION 2

Thyroid Hormone 2

Regulation of Thyroid Hormone Levels 2

Thyroid Hormone Receptors 4

Mouse Models of Thyroid Hormone Action 5

Thyroid Hormone Imbalances, Disease, and Therapy 6

THYROID HORMONE RECEPTORS AND CHOLESTEROL HOMEOSTASIS 7

Cholesterol Regulation 7

Effects of Thyroid Hormones on Cholesterol 9

THYROID HORMONES AND ENERGY HOMEOSTASIS 10

The Role of Thyroid Hormones in Metabolic Regulation 10

Adipose Tissue Types and Function 12

Thyroid Hormones in Adipose Tissues 14

CHAPTER 2 THYROID HORMONE RECEPTOR AGONISTS REDUCE SERUM CHOLESTEROL INDEPENDENT OF THE LDL RECEPTOR 16

INTRODUCTION 17

RESULTS 20

GC-1 Lowers Serum Cholesterol in LDLR$^{-/-}$ Mice 20

GC-1 Does Not Induce Alternative Lipoprotein Receptors, Including SR-BI 21

GC-1 Strongly Induces Cyp7a1, Resulting in Increased Bile Acid Synthesis and Secretion in LDLR$^{-/-}$Mice. 23

TR Agonists Reduce Serum Cholesterol More Effectively Than Statins in LDLR$^{-/-}$ Mice. 26

TR Agonists Reduce Plasma Lipids Despite Increased Hepatic VLDL and ApoB Secretion. 28

GC-1 Affects Bile Acid Synthesis Similarly in Mice That Possess Functional LDLRs. 29

Discussion 31

Materials and Methods 36

Animals 36

Animal Treatments 37

Lipid And Lipoprotein Analysis 37

Plasma C4 (7α-hydroxy-4-cholesten-3-one) Levels 38

Fecal Sterol Analysis 38

Immunoblotting 39

RNA Extraction and Real-time qPCR 39

Hepatic Triglyceride and ApoB Secretion Rate Determination 40

Statistical Analysis 40

CHAPTER 3 THYROID HORMONE RECEPTOR AGONISTS ELICIT A FUNCTIONAL CONVERSION OF WHITE TO BROWN FAT 41

INTRODUCTION 42

RESULTS 45

The TR Agonist GC-1 Elicits a BAT-like Program of Adaptive Thermogenesis in scWAT 45

GC-1-induced Browning of scWAT Coincides with Marked Thermogenesis and Metabolic Elevation 51
GC-1 Mediated Adaptive Thermogenesis is Independent of BAT Activity 57
In Addition To GC-1, T_3 Also Induces Adaptive Thermogenesis in scWAT of ob/ob Mice 60
GC-1 Mediated Thermogenesis is Dependent Upon White Adipose Tissue 63
WAT Browning by TR Agonists is at Least Partially Cell Autonomous 65
DISCUSSION 66
Materials and Methods 74
Animals 74
BAT Denervation 74
Hyperinsulinemic-Euglycemic Clamp 75
PET/CT Imaging 75
Primary Cell Culture 76
Oxygen Consumption Rate Analysis 77
Metabolic Phenotyping 78
Indirect Calorimetry 78
Acute Cold Challenge 78
RNA Extraction and Real-time qPCR 79
Mitochondrial DNA Content 79
Histology 79
Adipose Tissue Citrate Synthase Activity 80
Catecholamines 80
Immunoblotting 80
UCP1 Quantification 81

Statistical Analysis..... 81

CHAPTER 4 CONCLUDING REMARKS AND FUTURE PRESPECTIVES.....82

CHAPTER 5 REFERENCES.....87

Table of Figures

Figure 1-1. Iodothyronine deiodinase. 3

Figure 1-2. Schematic of TR isoform α and β 4

Figure 1-3. Schematic of cholesterol flux. 8

Figure 1-4. Brown and beige fat differentiation. 14

Figure 2-1. GC-1 reduces serum cholesterol and triglyceride levels in LDLR$^{-/-}$ mice. 21

Figure 2-2. Total hepatic cholesterol content and expression of hepatic lipoprotein receptors were unaffected by GC-1 in LDLR$^{-/-}$ mice. 22

Figure 2-3. GC-1 does not induce hepatic SR-BI protein. 23

Figure 2-4. Effect of GC-1 on bile acid synthesis and fecal excretion. 24

Figure 2-5. Effect of GC-1 on expression of hepatic and intestinal transporters involved in cholesterol homeostasis. 25

Figure 2-6. Effects of T_3, thyromimetics, and statins on serum cholesterol in LDLR$^{-/-}$ mice. 26

Figure 2-7. Effects of T_3, thyromimetics on lipoprotein receptors and cholesterol homeostasis genes in LDLR$^{-/-}$ mice. 27

Figure 2-8. GC-1 increases hepatic triglyceride and ApoB secretion rates. 28

Figure 2-9. GC-1 treatment elicits similar effects in mice with functional LDLRs. 29

Figure 2-10. GC-1 Treatment elicits similar effects in mice with functional LDLRs. 30

Figure 2-11. T_3 reduces serum cholesterol and affects bile acid synthesis in a fashion similar to GC-1. 31
Figure 3-1. Thermogenic gene expression in BAT, scWAT, epiWAT and muscle. 46
Figure 3-2. Similar levels of *Ucp1* transcript in scWAT of GC-1 as BAT. 47
Figure 3-3. GC-1 induces an increase in UCP1 protein in scWAT. 48
Figure 3-4. GC-1 induces mutlilocular lipid droplets in scWAT. 49
Figure 3-5. GC-1 induces increase in mitochondria and respiration in scWAT. 50
Figure 3-6. GC-1 induces an increase in metabolic rate and body temperature. 51
Figure 3-7. Dramatic weight and fat loss in ob/ob mice treated with GC-1. 52
Figure 3-8. No change in food intake or physical activity. 52
Figure 3-9. Weight loss is due solely to loss of adiposity. 53
Figure 3-10. GC-1 rescues thermogenic effect of ob/ob mice. 54
Figure 3-11. Improved insulin sensitivity assessed by hyperinsulinemic-euglycemic clamp. 55
Figure 3-12. Increases glucose tolerance of control and GC-1 treated ob/ob mice. 56
Figure 3-13. 18F-FDG PET/CT imaging of control and GC-1 treated ob/ob mice. 57
Figure 3-14. Glucose uptake in scWAT and BAT of control and treated ob/ob mice. 58

Figure 3-15. Thermogenic gene expression in scWAT and BAT of sham and BAT-denervated ob/ob mice. 58
Figure 3-16. Indistinguishable weight and fat loss and elevated body temperature between BAT-denervated and sham treated mice. 59
Figure 3-17. T_3 treatment induces similar weight and fat loss and increases body temperature. 60
Figure 3-18. Effects of T_3 on the thermogenic genes and UCP1 protein expression in scWAT. 61
Figure 3-19. T_3 increases mitochondria in scWAT. 62
Figure 3-20. Effects of T_3 on the thermogenic genes and UCP1 protein expression in BAT. 62
Figure 3-21. Correlation between rate of fat loss and initial fat mass. 63
Figure 3-22. GC-1 increases metabolic rate and elevates body temperature in DIO but not lean mice. 64
Figure 3-23. GC-1 induces browning of white adipocytes *in vitro*. 65
Figure 3-24. UCP1 protein per mouse and per adipose tissue. 68
Figure 3-25. Ucp1 transcript and estimated total UCP1 in scWAT and BAT of ob/ob and DIO mice 69

CHAPTER 1 INTRODUCTION

THYROID HORMONE: MECHANISM OF ACTION

Thyroid Hormone

Thyroid hormone actions are pleiotropic, involving the regulation of many physiological systems. Their actions are important in development as well as in adulthood. Thyroid hormones regulate the growth and maturation of many organs during embryonic development. During adulthood, the major function of thyroid hormone is the regulation of metabolism and function of many tissues, such as the liver, heart, skin, muscle, and adipose tissue (*1*).

Regulation of Thyroid Hormone Levels

As an important metabolic regulator, thyroid hormone levels must be tightly regulated to avoid metabolic dysfunction. The thyroid gland synthesizes two forms of thyroid hormone; the pro-hormone thyroxine (T_4) as well as a small amount of the active hormone triiodothyronine (T_3). Thyroid-stimulating hormone (TSH) stimulates the production of thyroid hormone in the thyroid gland. In a negative feedback loop, thyroid hormone represses the production of TSH in the hypothalamus and pituitary gland, referred to as the hypothalamus-pituitary-thyroid (HPT) axis (*2*).

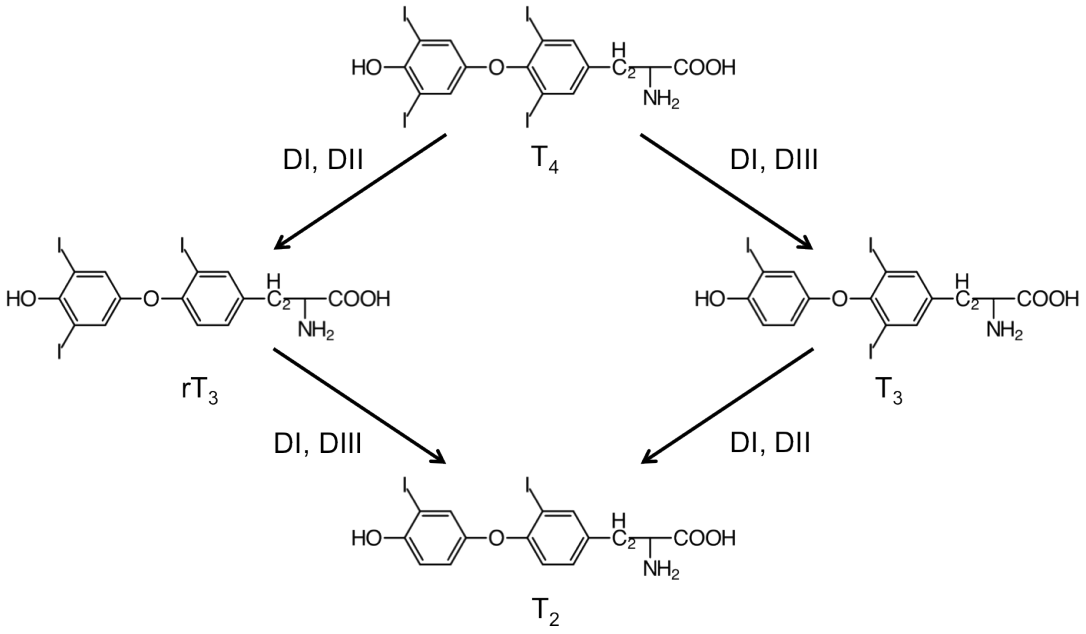

Figure 1-1. Iodothyronine deiodinase.
Thyroid hormones are activated and inactivated by specific chemical reactions involving iodothyronine deiodinases.

Intracellular levels of thyroid hormone are regulated within the target tissues by thyroid hormone transporters and monodeiodination enzymes. While it was previously assumed that the lipophilic property of thyroid hormone allowed the molecule to enter cells through passive diffusion, this view has changed since the discovery of specific thyroid hormone transporters. These thyroid hormone transporters, such as MCT8 and OATP14 (*3*), add an additional mechanism to regulate thyroid hormone levels within the cells. Intracellular levels of T_3 are fine tuned further by the action of type I and II deiodonases (Dio1 and Dio2) that convert T_4 to T_3 (Figure 1-1). Additionally, T_4 and T_3 can be inactivated by type I and III deiodonases (Dio1 and Dio3), which convert T_4 to reverse T_3 and T_3 to T_2 (*4*).

Thyroid Hormone Receptors

Thyroid hormone actions are initiated by interaction with the thyroid hormone receptors (TRs), which are members of the superfamily of nuclear receptors (*5*). TRs bind to specific DNA sequences (thyroid hormone response elements) to promote the regulation of specific target genes. Thyroid hormone binding leads to conformational changes in the receptors resulting in an exchange of corepressors for coactivators.

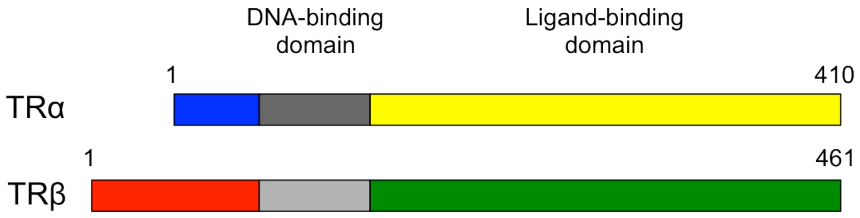

Figure 1-2. Schematic of TR isoform α and β .
The functional properties and length of TR α and β are indicated in above diagrams.

Two major TR isoforms are encoded by two distinct genes designated TRα and TRβ (Figure 1-2), encoded on human chromosome 17 and 3, respectively (*6*). The two TRs are highly homologous with the ligand-bind domain and DNA-binding domain being 86% and 82% identical, respectively. It is controversial whether the TRα and TRβ isoforms can compensate for each other but it appears that, depending upon context, TR isoforms can have both redundant roles and specific functions. The degree of redundancy seems to be largely

dependent upon the level of coexpression within a tissue. TRα is expressed ubiquitously in most tissues, with particularly high expression in the heart, while TRβ is expressed predominately in the liver and kidney (*7*).

Mouse Models of Thyroid Hormone Action

Several TR knockout and knockin mouse models have been generated to identify the specific actions of each TR isoform. While the first knockout mice did not show phenotypical abnormalities concerning adipose metabolism or alterations in energy balance (*8*–*10*), work with TR point mutations and dominant negative mutations identified phenotypes related to adipose tissue and energy balance (*11*–*14*). Overall, TRα seems to be required for proper thermogenesis, while TRβ regulates cholesterol metabolism. The TR double knockout mice as well as hypothyroid mice have decreased body temperature and basal metabolic rate (*15*, *16*). These mice, which are devoid of all TRs, also show growth retardation and delayed skeletal maturation along with increase in adiposity. Furthermore, the TRα P398H mutant knockin has increased visceral adiposity, hyperleptinemia, a fourfold increase in body fat, increased basal glucose and insulin, and impaired lipolysis (*17*). Thus far, nearly all reports have utilized whole body knockouts and knockins of the TR isoforms. Therefore, it is difficult to discern tissue-specific effects of individual isoforms.

Thyroid Hormone Imbalances, Disease, and Therapy

The connection between thyroid hormone and metabolism is exemplified by hyperthyroid and hypothyroid patients. Hyperthyroidism is a clinical disorder characterized by an excess production of thyroid hormone. Hyperthyroidism causes a hypermetabolic state characterized by increased energy expenditure and weight loss despite marked hyperphagia, tachycardia (increased heart rate) with possible atrial arrhythmias, muscle fatigue, anxiety, irritability, and preference for cold temperatures (*18*). On the other hand, hypothyroidism is when the thyroid gland does not produce enough thyroid hormone. Common symptoms of hypothyroidism are weight gain, high serum cholesterol, poor ability to tolerate cold and mood disturbances (*18*). Hypothyroidism is easily treated with thyroid hormone replacement therapy.

Patients with resistance to thyroid hormone (RTH) have elevated T_4 and T_3 and non-suppressed TSH. Despite the elevated thyroid hormone levels, patients with RTH do not exhibit the usual symptoms and metabolic consequences of excess thyroid hormone. RTH is generally caused by a mutation in TRβ that impairs thyroid hormone action, although defects in thyroid hormone transport (*19*, *20*) and metabolism (*21*) have recently been identified.

THYROID HORMONE RECEPTORS AND CHOLESTEROL HOMEOSTASIS

Cholesterol Regulation

TRs have a well established role in hepatic cholesterol metabolism and regulation of serum cholesterol levels. Cholesterol is the building block for cell membranes and essential for proper cell membrane permeability and fluidity. Cholesterol is also an important precursor molecule for many biochemical pathways such as vitamin D and steroid hormones. However, cholesterol in excess through a high-fat diet leads to the progression of atherosclerosis. Elevated levels of circulating low-density lipoprotein (LDL) cholesterol is associated with an increased risk of atherosclerotic cardiovascular disease (*22*). Conversely, decreased risk of cardiovascular disease is associated with the reductions in serum cholesterol levels that occur with the use of hepatic 3-hydroxy-3-methyl-glutaryl coenzyme A reductase (HMGCR) inhibitors, commonly known as statins (*22*).

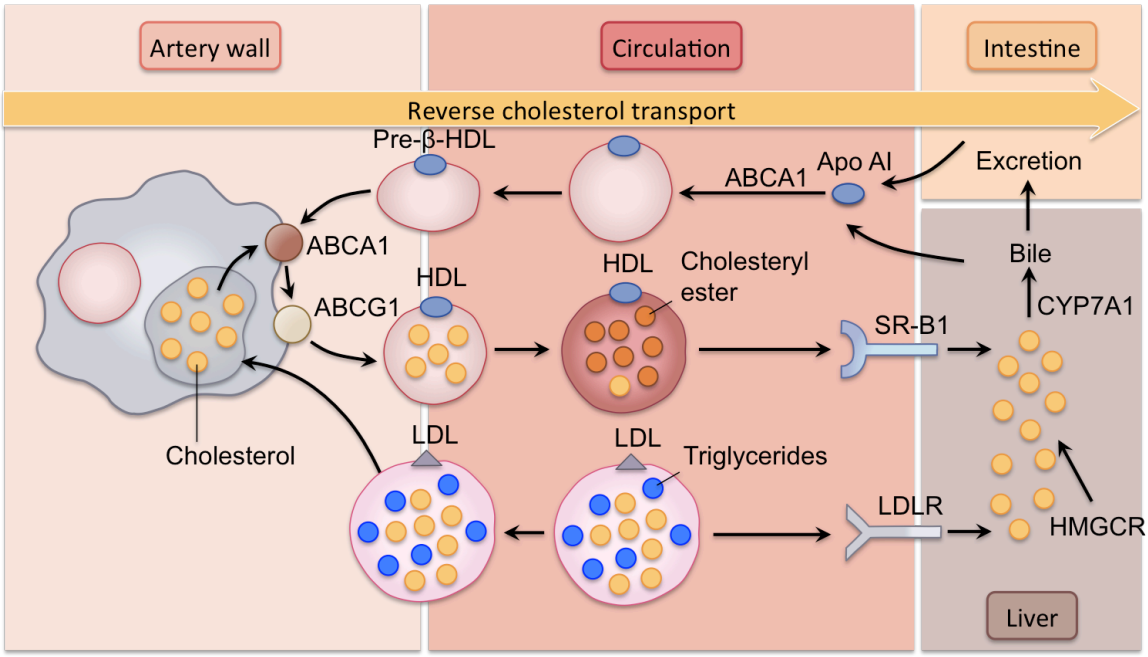

Figure 1-3. Schematic of cholesterol flux.
LDL–cholesterol particles can deposit cholesterol in the artery wall to form plaques or can be reabsorbed into the liver through interactions with LDLR. For the HDL pathway, precursor particles containing apolipoprotein A1 (APOA1) are secreted into the circulation, where they pick up cholesterol from atherosclerotic plaques and other sources to become mature HDL particles. HDL particles are taken up by the liver through interactions with liver HDL receptors, scavenger receptor B1 (SR-B1). Liver cholesterol content is regulated by the rate of synthesis and the rate of conversion to bile acids, which are secreted into the intestine. The enzymes 3-hydroxy-3- methyl-glutaryl-CoA reductase (HMGCR) and cytochrome P450 7A1 (CYP7A1) regulate important steps in cholesterol metabolism.

Regulation of cholesterol homeostasis is complex and only parts of cholesterol regulation are understood, see Figure 1-3. Intracellular cholesterol levels are sensed by the sterol-regulatory element binding protein (SREBP) (*23*). When cholesterol levels are low, SREBP translocates into the nucleus, where it acts as a transcription factor and stimulates transcription of many genes including HMGCR and LDL receptor (LDLR). HMGCR is the rate-limiting enzyme in the synthesis of cholesterol. LDLR scavenges the blood for LDL-cholesterol and

takes up cholesterol into the cell. When cholesterol levels are high, HMGCR is degraded.

Cholesterol from peripheral tissues is transported back to the liver via high-density lipoprotein (HDL) through a process called reverse cholesterol transport (RCT). HDL-cholesterol protects against cardiovascular disease by removing cholesterol from atherosclerotic plaques, which is then taken up into the liver via the HDL scavenger receptor B1 (SR-B1). HDL-associated cholesterol can then be converted to bile acids by cholesterol 7α-hydroxylase (Cyp7a) and excreted.

Effects of Thyroid Hormones on Cholesterol

Hypothyroidism is associated with hypercholesterolemia in humans and animals due to a reduced clearance of serum LDL-cholesterol resulting from decreased LDLR (*24*–*27*). The cholesterol-lowering effects of thyroid hormone replacement therapy in hypothyroid patients have been previously described (*28*). Although thyroid hormone can lower serum cholesterol, the treatment of hypercholesterolemia by thyroid hormone is limited due to deleterious cardiac and other side effects (*29*). However, synthetic thyroid hormone analogues, which have receptor-subtype selective and liver-selective activities and are often referred to as thyromimetics, have been developed for cholesterol lowering (*30*–*33*). Several thyromimetics have been shown to possess cholesterol-lowering actions in mice, monkeys and humans (*30*–*33*).

The activation of TR clearly causes a decrease in LDL cholesterol, however the mechanism(s) by which TR activation reduces serum cholesterol is not well understood. While TR agonism has been shown to affect multiple pathways involved in cholesterol homeostasis (*34*–*36*), the relative importance of individual factors in mediating serum cholesterol reduction is unclear. Increased LDLR expression is the principal mechanism by which many drugs (including statins) lower cholesterol (*37*), and the TRs have been shown previously to induce LDLR (*34*, *38*, *39*)*;* it is perhaps not surprising that this action is the most often-described mechanistic rationale for cholesterol reduction by the TRs (*28*). Additionally, thyroid hormone analogues also accelerate clearance of cholesterol by the liver by increasing SR-B1, increasing the activity of CYP7A1, and increasing fecal excretion of cholesterol as bile acids (*38*, *40*, *41*).

THYROID HORMONES AND ENERGY HOMEOSTASIS

The Role of Thyroid Hormones in Metabolic Regulation

It is well known that thyroid hormones are involved in the regulation of thermogenesis, body temperature, and energy balance (*42*). In humans, hypothyroidism is associated with weight gain and hypersensitivity to cold while

in hyperthyroidism is patients experience weight loss and difficulty tolerating the heat (*18*).

Generally, thyroid hormone-induced thermogenesis is attributed to BAT, however, a full understanding of the mechanisms by which thyroid hormone increases metabolic rate remains unclear (*42*). The role of thyroid hormone in BAT is evident in *Dio2*$^{-/-}$ mice, which are hypothermic due to impaired BAT thermogenesis, while the administration of T_3 rescues the thermogenic defects (*43*). Thyroid hormones have been shown to increase uncoupling protein-1 (UCP1) expression, mitochondrial number, oxidative phosphorylation rates and thermogenesis in BAT (*44*, *45*). Additionally, thyroid hormone upregulates genes involved in mitochondrial respiration (*46*).

In addition to BAT-mediated thermogenesis, it is generally accepted that other tissues also contribute to thyroid hormone-induced thermogenesis. Thyroid hormone has been shown to induce sarcoplasmic reticulum calcium ATPase (SERCA) in muscle, which induces Ca^{2+} cycling and increase energy expenditure leading to heat production (*47*, *48*). Additionally, thyroid hormone induces futile cycles in glucose and fat metabolism, in which substrates and products are interconverted, leading to heat production (*49*–*51*). Thus, although thyroid hormone plays a clear role in thermogenesis and metabolic regulation, it is not

fully apparent how much each of these actions contributes to the effects of thyroid hormone on systemic metabolism.

Adipose Tissue Types and Function

Thyroid hormone increases systemic metabolism and energy demand, which affects adipose tissue biology. Adipose tissue is specialized in the transport, synthesis, and storage of lipids. Although excess caloric intake and decreased energy expenditure promote overall weight gain, visceral adiposity is particularly associated with cardiometabolic risk (*52*). There are two types of adipose tissue: white adipose tissue (WAT) and brown adipose tissue (BAT). While WAT functions to store energy in the form on triglycerides and comprises a reservoir of energy to be use in times of caloric demand, BAT can dispose of excess energy by converting it to heat (*53*–*55*).

WAT is morphologically characterized by a single large lipid droplet, which fills the intracellular space. There are two types of WAT, subcutaneous and visceral fat. While these types are based on anatomical location, there are differences in lipolytic sensitivity, insulin sensitivity, and inflammatory tendency. Increase in visceral fat is associated with elevated risk of metabolic dysfunction such as insulin resistance, type 2 diabetes and cardiovascular disease (*52*, *56*–*60*). While subcutaneous fat is associated with improvement of insulin sensitivity, and lowered risk of type 2 diabetes and atherosclerosis (*61*–*65*). However the

molecular mechanism for these differences between the WAT depots is still unclear.

BAT is specialized in non-shivering adaptive thermogenesis and functions to generate heat in exchange for calories. BAT is morphologically characterized by multilocular lipid droplets and abundant mitochondria. The dissipation of heat is generated by UCP1, which uncouples oxidative phosphorylation, thereby dissipating the proton gradient and leading to the generation of heat instead of ATP. Its exceptional ability to burn excess calories as heat is considered anti-obesogenic (*66*, *67*). While BAT was thought to be found only in hibernating animals, small rodents, and newborns, recent studies have shown that BAT exists in humans and is associated with leanness (*68*–*72*). This has renewed interest in the pharmacological potential of the anti-obesogenic actions of BAT.

Recent studies have shown the ability to impart BAT-like function within WAT of rodents and humans (*73*–*76*). These brown-like cells that arise within WAT depots have come to be called recruitable brown fat cells, brown-in-white (brite) cells, and beige cells. This process of browning of WAT is enhanced by cold adaptation or β-adrenergic stimulation (*77*–*82*). The brown-like transformation of WAT is most predominant in the subcutaneous depot, whereas visceral fat is less susceptible to browning (*77*, *79*, *83*, *84*). The mechanism by which beige cells emerge is not yet clear, although a recent lineage-tracing study suggested that

beige adipocytes arise from distinct progenitor cells residing in WAT depots (*85*) (Figure 1-4). Regardless of mechanism, the ability to functionally convert white into brown-like adipocytes appears to hold promise as a method to combat obesity and diabetes.

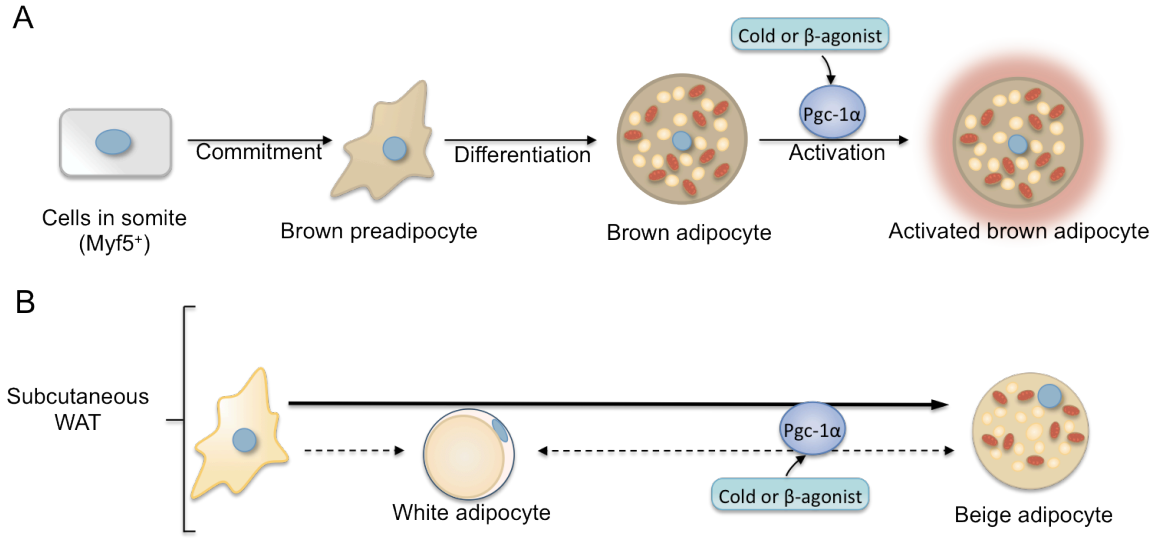

Figure 1-4. Brown and beige fat differentiation.
(A) Brown adipocytes are derived from a *Myf5*-expressing progenitor population. Thermogenesis in mature brown adipocytes is activated by norepinephrine (NE), a β3 agonist, released from sympathetic neurons. NE signals through β-adrenergic receptors to increase the expression and activity of Pgc-1α, a transcriptional coactivator that coordinates gene programming in response to activation. (B) In inguinal fat, β-adrenergic stimulation triggers predominantly *de novo* differentiation of precursor cells (large arrow). There are also possibilities that under some conditions mature white fat cells can transdifferentiate into beige cells (small dashed arrow).

Thyroid Hormones in Adipose Tissues

As a key modulator of energy balance and thermogenesis, excess thyroid hormone elicits substantial changes in lipid metabolism (*32*, *42*). Thyroid hormone modulates the development and metabolism of adipose tissue in both

physiological and pathological conditions. All TR isoforms are expressed in WAT and BAT, with TRα being the predominant isoform. Studies have shown thyroid hormones play essential role in BAT physiology and are necessary for full thermogenic response. Thyroid hormones also induce lipolysis in WAT, which is generally thought to be indirect and due to an increase in systemic metabolic rate and energy demand. However, a recent study has suggested a direct effect of thyroid hormones in WAT metabolism due to the induction of Ucp1 expression (*45*). Regardless of mechanism, TR activation clearly elicits fat loss. Thus, thyroid hormone analogues have long been pursued as anti-obesity agents. These compounds have been shown to induce fat loss and elevate metabolic rate in mice and rats (*32*), suggesting that the TR agonists could hold potential as anti-obesity therapeutics.

CHAPTER 2 THYROID HORMONE RECEPTOR AGONISTS REDUCE SERUM CHOLESTEROL INDEPENDENT OF THE LDL RECEPTOR

The majority of cholesterol reduction therapies, such as the statin drugs, work primarily by inducing the expression of hepatic LDLRs, rendering these therapeutics only partially effective in animals lacking LDLRs. While thyroid hormones and their synthetic derivatives, often referred to as thyromimetics, have been clearly shown to reduce serum cholesterol levels, this action has generally been attributed to their ability to increase expression of hepatic LDLRs. Here we show for the first time that the thyroid hormone T_3 and the TRβ selective agonists GC-1 and KB2115 are capable of markedly reducing serum cholesterol in mice devoid of functional LDLRs by inducing Cyp7a1 expression and stimulating the conversion and excretion of cholesterol as bile acids. Based on this LDLR-independent mechanism, thyromimetics such as GC-1 and KB2115 may represent promising cholesterol lowering therapeutics for the treatment of diseases such as homozygous familial hypercholesterolemia, a rare genetic disorder caused by a complete lack of functional LDLRs, for which there are limited treatment options as most therapeutics are only minimally effective.

INTRODUCTION

Familial Hypercholesterolemia (FH) is a genetic disorder characterized by elevated levels of serum cholesterol and associated with early onset cardiovascular disease. FH is a manifestation of a misfunctional allele encoding the low density lipoprotein receptor (LDLR), the primary receptor responsible for

clearing cholesterol laden low-density lipoprotein (LDL) particles from the blood. Although FH, in its heterogenous form, affects 1 in 500 people (*86*); it can generally be treated with HMGCR inhibitors, a class of drugs collectively referred to as the statins. However, approximately 1 in 1 million people are affected by homozygous FH (hFH) and possess essentially no functional LDLRs. These patients manifest severe and widespread atherosclerosis leading to coronary events at ages as young as 1-2 years and untreated hFH generally results in death due to cardiovascular disease, commonly in the teen years. While conventional treatment can extend the life expectancy of hFH patients, longer term survival often requires unusual methods, such as liver transplantation or repeated plasmapheresis, that are generally not available to many patients. Since most common therapies utilized to reduce serum cholesterol levels, such as the statins and bile acid sequestrants, ultimately rely upon a secondary induction of hepatic LDLRs to mediate the uptake of cholesterol containing lipoproteins from the plasma into the liver, their utility in treating hFH is limited. Thus new therapeutic options for the treatment of hFH are sorely needed.

Although endogenous thyroid hormones, such as T_3, can lower serum cholesterol, their use in the treatment of hypercholesterolemia is limited due to deleterious cardiac and other side effects. This has led to development of thyromimetics, thyroid hormone analogues designed to maintain the beneficial effects of thyroid hormones, such as cholesterol reduction and weight loss,

without undesirable side effects (*87*). As a class, thyromimetics have been shown to lower serum cholesterol levels in rodents, monkeys, and humans. While it is clear that thyroid hormones and thyromimetics reduce serum cholesterol levels, the mechanism behind this reduction is less apparent. TR agonists have been reported to reduce plasma cholesterol levels via induction of several different pathways that include increasing bile acid synthesis via the induction of Cyp7a1 (*38*, *40*, *41*) and increasing reverse cholesterol transport by increasing expression of the HDL receptor SR-BI (*40*, *41*). However, the most notable rationale has been that thyroid hormones can stimulate expression of the LDLR (*34*, *38*, *39*). In support of this mechanistic view, all reports describing the use of T_3 or thyromimetics in $LDLR^{-/-}$ mice have found the compounds to be ineffective at lowering plasma cholesterol levels in this genetic background (*38*, *41*), despite the same compounds demonstrating efficacy in mice that possessed functional LDLRs.

GC-1 is a thyromimetic that has been studied extensively and has been shown to lower LDL cholesterol in multiple species (*32*, *88*). A previous report described that GC-1 was able to reduce serum cholesterol by 25% in wild-type mice, with no accordant increase observed in LDLR levels, and this effect was attributed to increases in reverse cholesterol transport mediated by increased expression of the HDL receptor, SR-BI (*40*). Given that GC-1 was able to reduce serum cholesterol in the absence of any apparent increase in LDLR levels, it seemed

reasonable to determine whether this compound retained at least partial efficacy in mice lacking functional LDLRs. Here, we show that the thyroid hormone T_3 and the thyromimetics GC-1 and KB2115 are potent and effective reducers of serum LDL cholesterol in $LDLR^{-/-}$ mice and present evidence to show that this effect is related to an increased conversion of cholesterol to bile acids and a subsequent increase in bile acid secretion. We propose that thyromimetics may represent a novel therapeutic approach to the treatment of hFH.

RESULTS

GC-1 Lowers Serum Cholesterol in $LDLR^{-/-}$ Mice

$LDLR^{-/-}$ mice fed a high fat, high cholesterol diet exhibited serum cholesterol levels that were elevated approximately 10-fold relative to wild type mice fed a similar diet (Figure 2-1A). Somewhat unexpectedly, supplementation of diets with the thyromimetic GC-1 triggered a rapid and marked decrease in serum cholesterol and triglycerides (Figure 2-1, A and B), with both being reduced to about one third of their pre-treatment levels in 7 days. FPLC fractionation of cholesterol containing lipoproteins indicated that the reduction in serum cholesterol resulted primarily from a reduction in LDL cholesterol (Figure 2-1C), as little to no changes were apparent in the cholesterol content of VLDL and HDL fractions. Thus, GC-1 can induce dramatic LDL cholesterol-lowering in the absence of LDL receptors in mice.

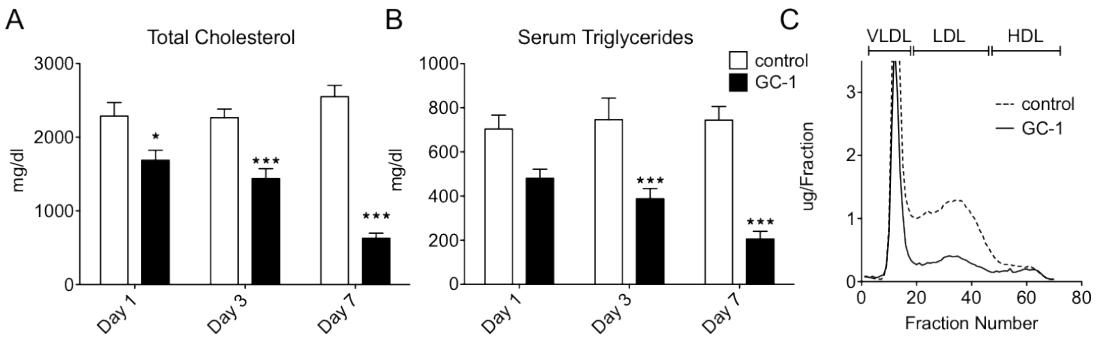

Figure 2-1. GC-1 reduces serum cholesterol and triglyceride levels in LDLR$^{-/-}$ mice.
Male LDLR$^{-/-}$ mice were administered GC-1 (4.8 mg/kg-diet) in a western diet containing 0.2% cholesterol or control diet lacking GC-1 (*n* = 6). Blood samples were collected at the times indicated and assayed for serum cholesterol (A) and triglycerides (B). (C) Size exclusion fractionation of serum lipoproteins from mice administered GC-1 for 10 days (blood from 5 animals was pooled for each trace). Data are mean ± s.e.m. **P* < 0.05, ****P* < 0.001.

GC-1 Does Not Induce Alternative Lipoprotein Receptors, Including SR-BI.

The majority of cholesterol reduction therapies, including the statins, work via an SREBP mediated increase in LDLR levels, which results in increased LDLR-dependent uptake of LDL cholesterol from the plasma compartment into the liver. For example, transgenic mice that overexpress SREBP-1a have reduced serum cholesterol levels despite an increased rate of cholesterol synthesis due to a 6-fold increase in liver cholesterol storage that is mediated via the LDLR (*35*). To assess whether GC-1 caused a similar net transfer of cholesterol from the serum into hepatocytes of LDLR$^{-/-}$ mice, perhaps via the induction of alternative hepatic lipoprotein receptors, liver cholesterol levels were measured. Total hepatic cholesterol content was unaffected by GC-1 and expression levels of alternative hepatic lipoprotein receptors were unchanged following GC-1 treatment (Figure

2-2, A and B). Thus, the GC-1 dependent reduction in serum cholesterol was not due to a net increase in liver cholesterol storage.

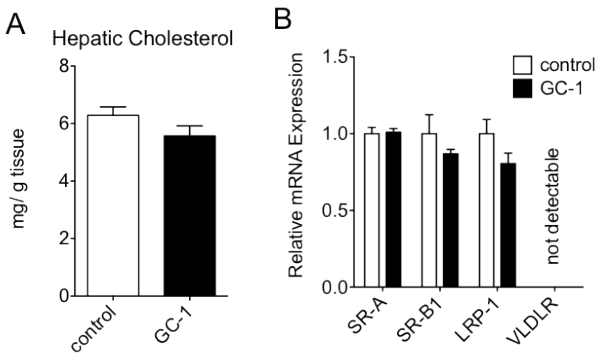

Figure 2-2. Total hepatic cholesterol content and expression of hepatic lipoprotein receptors were unaffected by GC-1 in LDLR$^{-/-}$ mice.
Hepatic cholesterol and lipoprotein receptor expression were assessed from livers collected from LDLR$^{-/-}$ mice treated with GC-1 for 10 days (*n* = 6).). Data are mean ± s.e.m.

Several reports have suggested that thyroid hormones and GC-1 reduce serum cholesterol by increasing hepatic expression of the HDL receptor, SR-BI, and stimulating aspects of reverse cholesterol transport through the HDL pathway (*40*, *41*). However, GC-1 treatment did not induce expression of SR-BI at either the gene or protein level in LDLR$^{-/-}$ mice (Figure 2-2B and 2-3). Given the absence of effects on HDL cholesterol levels and the HDL receptor, SR-BI, our data are largely inconsistent with the idea that marked GC-1 dependent reductions in LDL cholesterol levels in LDLR$^{-/-}$ mice are related to changes in HDL uptake.

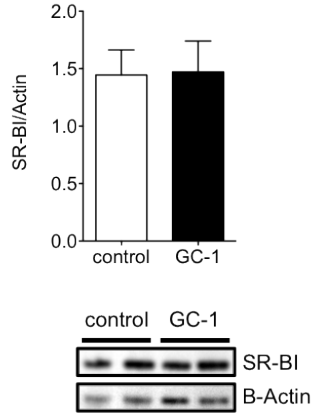

Figure 2-3. GC-1 does not induce hepatic SR-BI protein.
SR-BI protein levels were measured from male LDLR$^{-/-}$ mice treated with GC-1 for 10 days (*n* = 6). Data are mean ± s.e.m.

GC-1 Strongly Induces Cyp7a1, Resulting in Increased Bile Acid Synthesis and Secretion in LDLR$^{-/-}$Mice.

Although we were unable to find mechanistic evidence of GC-1 dependent increases in cholesterol uptake into the liver, subsequent steps of reverse cholesterol transport, in particular numerous mediators of bile acid synthesis and excretion, were strongly affected by GC-1 treatment. Hepatic expression of Cyp7a1, the enzyme responsible for the rate-limiting step in the synthesis of bile acids from cholesterol, was increased 7-fold following GC-1 treatment (Figure 2-4A). Consistent with the large increase in Cyp7a1 levels, serum levels of 7alpha-hydroxy-4-cholesten-3-one (C4), a marker of bile acid synthesis and a physiologic indicator of Cyp7a1 activity (*89*), were increased nearly 5-fold following GC-1 treatment (Figure 2-4B) and fecal excretion of bile acids was increased 2.5-fold (Figure 2-4C). In accordance with increased synthesis of bile

acids and an expansion of the bile acid pool, expression levels of I-BABP, a reporter of intestinal bile acid levels (*90*), was increased approximately 3-fold (Figure 2-4D). ASBT, which is responsible for reabsorption of bile acids in the ileum and whose inhibition has been shown to increase fecal bile acid excretion (*91*), was significantly reduced by GC-1 (Figure 2-4E).

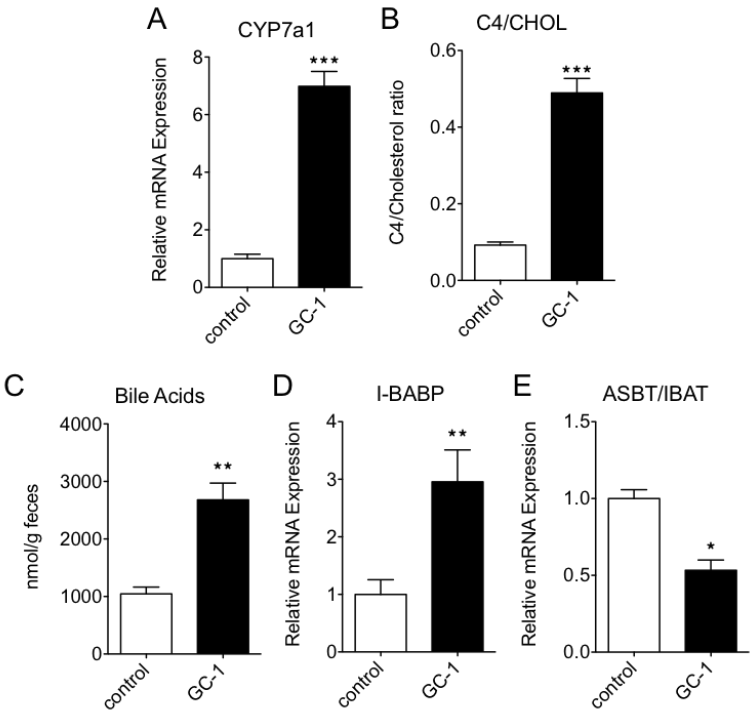

Figure 2-4. Effect of GC-1 on bile acid synthesis and fecal excretion.
Male LDLR$^{-/-}$ mice were administered GC-1 (0.8 mg/kg-diet) in a western diet containing 0.2% cholesterol or control diet lacking GC-1. Hepatic Cyp7a1 expression (A) and serum C4 levels (B) were measured after 10 days of treatment. (C) Feces were collected from days 5-8 of treatment and analyzed for bile acids. (D,E) Intestinal expression of I-BABP and ASBT of mice treated with GC-1 for 10 days (n = 4-5 per group) (*P<0.05, **P<0.01, ***P<0.001)

Although hepatic ABCB4, which is involved in bile acid and phospholipid excretion, was induced by GC-1, other hepatic transporters commonly implicated in cholesterol uptake and efflux, were unaltered (Figure 2-5A). Intestinal transporters including the LXR and FXR target genes ABCG5/8 (*92*), and OSTa/b (*93*), whose induction has been linked to increased cholesterol and bile efflux were either unaltered or decreased (Figure 2-5B). Although decreased expression of intestinal ABCG5/8 would be expected to increase the uptake of neutral sterols (*92*, *94*), the net excretion of neutral sterols was unaltered (Figure 8C), indicating that compensatory mechanisms, such as the actions of hepatic ABCG5/8 whose levels were unchanged, offset any increase in the uptake of neutral sterols. Collectively, these data suggest that the induction of Cyp7a1 by GC-1 strongly affects bile acid synthesis and excretion pathways evoking a net flux of cholesterol from the plasma compartment into the bile pool as bile acids, which are then excreted in the feces.

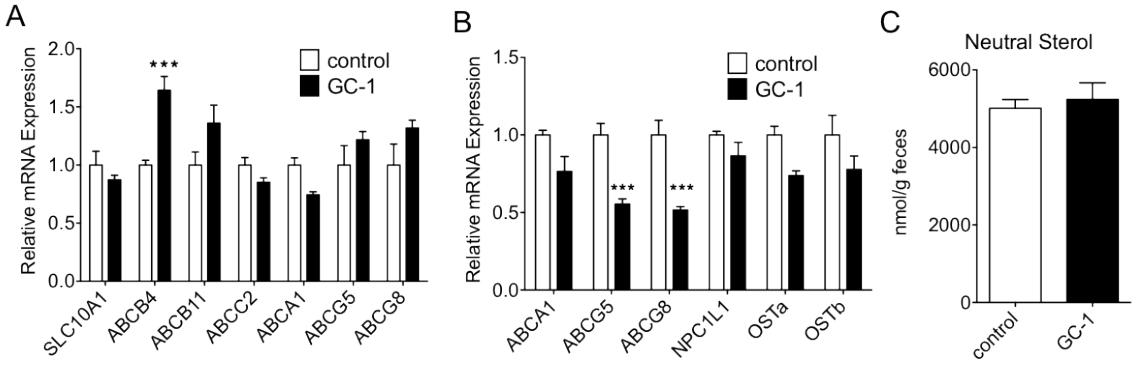

Figure 2-5. Effect of GC-1 on expression of hepatic and intestinal transporters involved in cholesterol homeostasis.
Gene expression of cholesterol transporters in liver (A) or ileum (B) sections of mice treated with GC-1 for 10 days (n = 4–5). Feces were collected from days 5-8 of treatment and analyzed for neutral sterols. Data are mean ± s.e.m. ***P < 0.001.

TR Agonists Reduce Serum Cholesterol More Effectively Than Statins in LDLR$^{-/-}$ Mice.

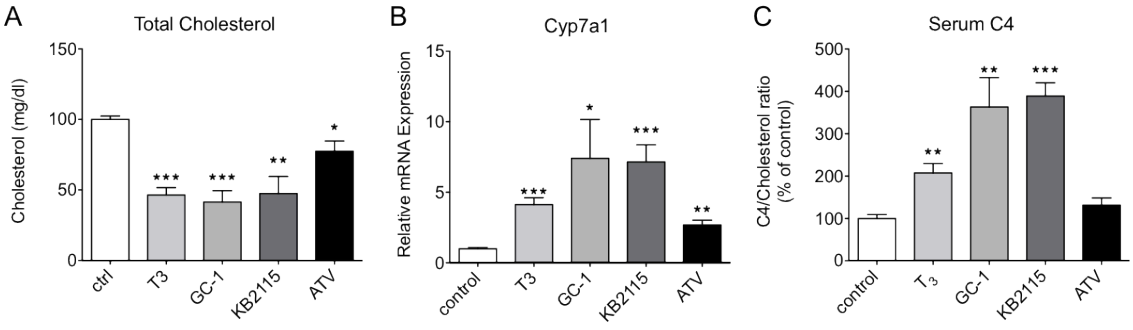

Figure 2-6. Effects of T_3, thyromimetics, and statins on serum cholesterol in LDLR$^{-/-}$ mice. Male LDLR$^{-/-}$ mice were administered GC-1 (0.8 mg/kg-diet) in a western diet containing 0.2% cholesterol or control diet lacking GC-1 (n = 4–5). Hepatic Cyp7a1 expression (A) and serum C4 levels (B) were measured after 10 days of treatment. (C) Feces were collected from days 5-8 of treatment and analyzed for bile acids. Intestinal expression of I-BABP (D) and ASBT (E) of mice treated with GC-1 for 10 days. Data are mean ± s.e.m. *P < 0.05, **P < 0.01, ***P < 0.001.

To determine whether cholesterol reduction in LDLR$^{-/-}$ mice was a property unique to GC-1 we compared the efficacy of GC-1 to that of another thyromimetic, KB2115, the thyroid hormone T_3, as well as atorvastatin, the last of which represents one of the most powerful statin drugs (*95*). Mice treated with either GC-1, KB2115, or T_3 for 10 days exhibited similar levels of cholesterol reduction (Figure 2-6A), indicating that the ability to significantly reduce serum cholesterol in the absence of functional LDLRs extends beyond GC-1, and is perhaps a general capability of all TR agonists. All three TR agonists increased Cyp7a1 expression between 4 and 7-fold and evoked a correspondent increase in bile acid synthesis, as indicated by increased plasma C4 levels (Figure 2-6, B and C). Consistent with the idea that the statins and TR agonists utilize distinct

mechanisms of cholesterol reduction, T_3 and the thyromimetics were more effective than atorvastatin at reducing serum cholesterol in $LDLR^{-/-}$ mice and only the TR ligands increased bile acid synthesis, as indicated by serum C4 levels. Expression levels of hepatic lipoprotein receptors and genes involved in cholesterol homeostasis were affected similarly by all TR agonists (Figure 2-7, A and B). Notably, SR-BI was repressed by all treatments, further arguing against SR-BI-mediated reverse cholesterol transport playing a key role in the observed cholesterol reduction.

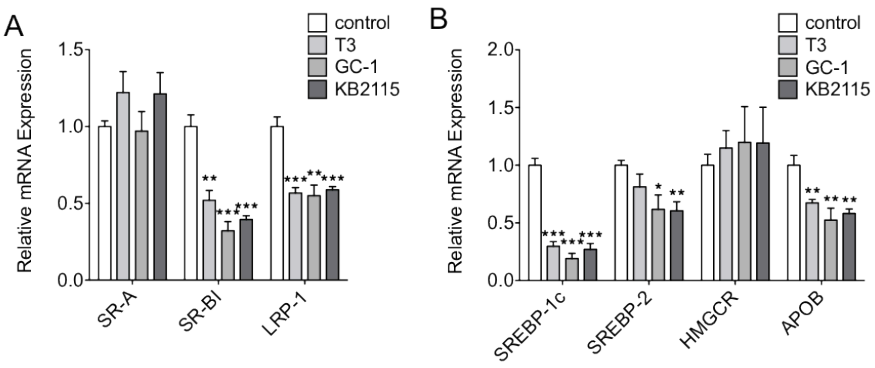

Figure 2-7. Effects of T_3, thyromimetics on lipoprotein receptors and cholesterol homeostasis genes in $LDLR^{-/-}$ mice.
Changes in expression of hepatic of lipoprotein receptors (A) and regulatory genes (B) were measured from $LDLR^{-/-}$ mice fed a western diet containing 0.2% cholesterol and treated with either 0.3 mg/kg T_3, 0.3 mg/kg KB2115, 0.3 mg/kg GC-1, or vehicle administered via i.p. injection for 10 days (n = 5). Data are mean ± s.e.m. *P < 0.05, **P < 0.01, ***P < 0.001.

TR Agonists Reduce Plasma Lipids Despite Increased Hepatic VLDL and ApoB Secretion.

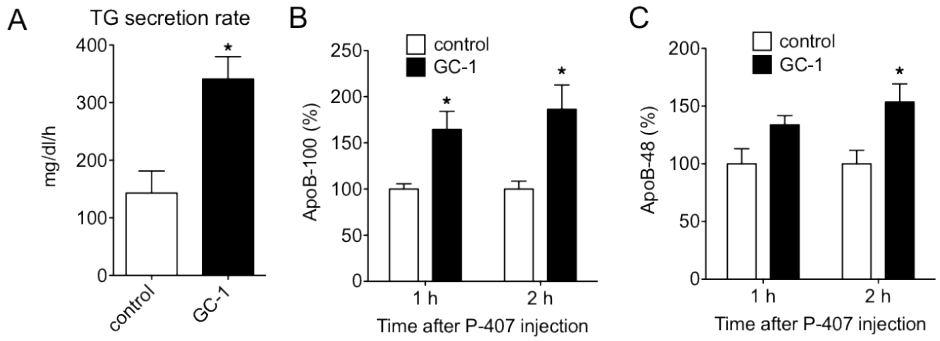

Figure 2-8. GC-1 increases hepatic triglyceride and ApoB secretion rates.
Male LDLR$^{-/-}$ mice were administered GC-1 (4.8 mg/kg-diet) in a western diet containing 0.2% cholesterol or control diet lacking GC-1 for 10 days (*n* = 3–4). After a 4 h fast, mice were injected with poloxamer 407 (P-407) and [^{35}S]-methionine. Blood was collected at time 0, 1, and 2 hr and assayed for triglycerides (TG) (A), ApoB-100 (B), and ApoB-48 (C). Data are mean ± s.e.m. *P < 0.05.

That hepatic cholesterol levels did not decrease despite markedly increased rates of bile acid synthesis and fecal excretion suggests that a compensatory mechanism must be responsible for preventing a reduction in hepatic cholesterol. Treatment with T_3, GC-1, or KB2115 lowered hepatic expression of the lipogenic regulators SREBP-1c and SREBP-2 and decreased ApoB mRNA levels, leading us to hypothesize that the decreased hepatic secretion of ApoB containing lipoproteins may account for the reduced levels of serum lipids as well as the maintenance of hepatic cholesterol. The rate of accumulation of triglycerides and nascent ApoB in the blood was determined following the coadministration of [^{35}S]-methionine and the lipoprotein lipase inhibitor poloxamer 407. Hepatic secretion of both triglycerides and [^{35}S]-methionine-labeled ApoB increased

strongly following GC-1 treatment (Figure 2-8). Although unexpected, these results are consistent with previous reports demonstrating that T_3 treatment and Cyp7a1 overexpression increase hepatic ApoB and triglyceride secretion (*96–98*), despite both TH action and Cyp7a1 activity being clearly associated with net reductions in serum ApoB containing lipoproteins. Thus, the relationship between thyroid hormones and their hepatic target Cyp7a1 with serum lipoprotein levels is likely complex.

GC-1 Affects Bile Acid Synthesis Similarly in Mice That Possess Functional LDLRs.

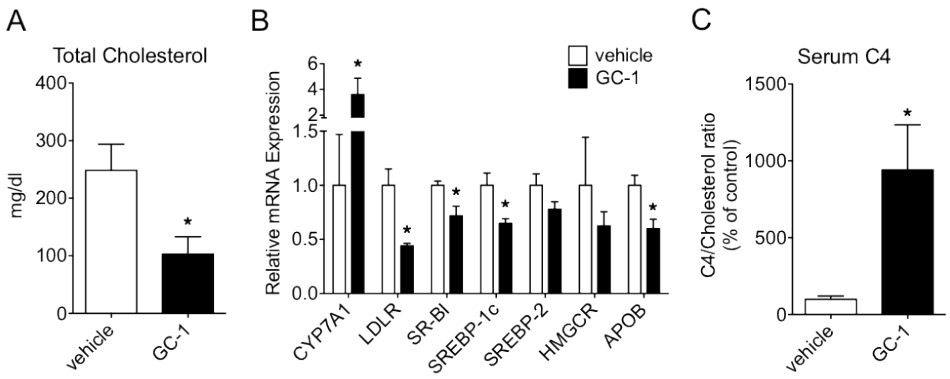

Figure 2-9. GC-1 treatment elicits similar effects in mice with functional LDLRs.
Male C57 mice fed a western diet containing 0.2% cholesterol were administered 0.3 mg/kg/d GC-1 or vehicle via i.p. injection for 10 days (n = 4–5). Changes in serum cholesterol (A), hepatic gene expression (B), serum C4 levels (C) were measured. Data are mean ± s.e.m. *P < 0.05.

In order to assess whether TR agonists utilize distinct mechanisms of cholesterol reduction in $LDLR^{-/-}$ mice and wild-type mice that possess functional LDLRs, C57 mice fed a western diet were treated with either GC-1 or T_3. GC-1 treatment

resulted in a complete normalization of serum cholesterol, markedly increased hepatic Cyp7a1 expression and rate of bile acid synthesis, and altered hepatic gene expression (Figure 2-9, A-C) in a manner remarkably similar to that seen when LDLR$^{-/-}$ mice were administered GC-1 (Figure 2-6).

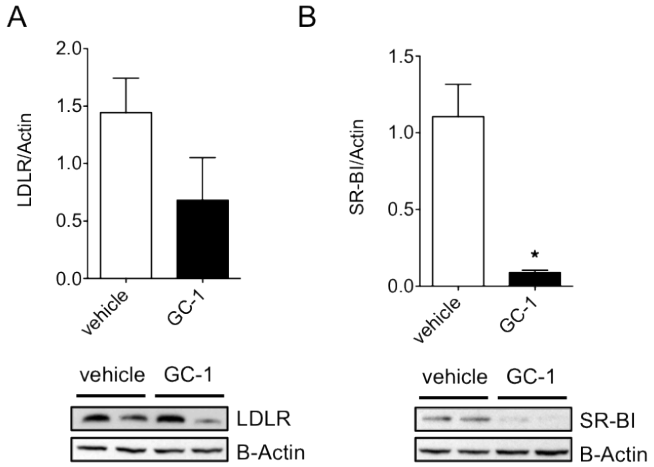

Figure 2-10. GC-1 Treatment elicits similar effects in mice with functional LDLRs.
Changes in LDLR (A) and SR-BI protein (B) were measured from male C57 mice fed a western diet containing 0.2% cholesterol were administered 0.3 mg/kg/d GC-1 or vehicle via i.p. injection for 10 days (n = 4–5). Data are mean ± s.e.m. *P < 0.05.

GC-1 led to a significant down-regulation of the hepatic lipoprotein receptors LDLR and SR-BI, at both the gene and protein level (Figure 2-9B and Figure 2-10), making it unlikely that cholesterol uptake by either receptor was responsible for the decrease in serum cholesterol. Treatment with T_3 at a level similar to that tolerated by LDLR$^{-/-}$ mice proved to be toxic to this strain, precluding detailed analysis of the data. Qualitatively, however, T_3 appeared to act in a manner analogous to GC-1 (Figure 2-11). These data suggest that the hepatic induction

of the lipoprotein receptors LDLR and SR-BI is likely unnecessary for the cholesterol lowering effects of TR activation.

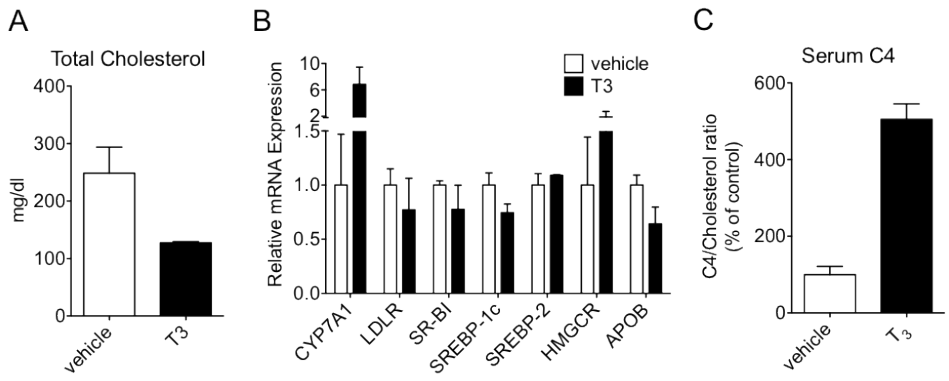

Figure 2-11. T_3 reduces serum cholesterol and affects bile acid synthesis in a fashion similar to GC-1.
Male C57Bl6 Mice were treated with 0.3 mg/kg-day T_3 administered via i.p. injection for 10 days, which proved to be toxic to this strain, resulting in morbidity or mortality to most treated animals. Serum cholesterol (A), hepatic gene expression (B) and serum C4 levels (C) were measured for the surviving animals (*n* = 2). Data are mean ± s.e.m. Statistical analysis was not performed due to the small number of animals.

Discussion

In this study, we report that the thyroid hormone T_3 and two TRβ-selective thyromimetics, GC-1 and KB2115, bring about marked reductions in serum total and LDL cholesterol in $LDLR^{-/-}$ mice, which lack functional LDL receptors. Our results suggest that cholesterol reduction in these mice is mediated primarily via the induction of Cyp7a1, leading to increased fecal excretion of cholesterol as bile acids, and does not require the action of alternative lipoprotein receptors such as the HDL receptor SR-BI. This finding suggests that current models,

which generally suggest that the effects of thyroid hormones and thyromimetics upon serum cholesterol are mediated principally by the increased expression of the hepatic lipoprotein receptors LDLR and SR-BI, are, at best, incomplete.

The actions of many commonly used cholesterol lowering therapeutics, such as the statins, bile sequestrants, and the NPC1L1 inhibitor ezetimibe, are mediated in large part by increased expression of LDLRs. Since thyroid hormones have been shown to induce the LDLR similarly, it is not surprising that increased LDLR expression is the mechanism most common ascribed to cholesterol reduction by thyroid hormones (*28*). Although several other mechanisms of cholesterol reduction by thyroid hormones have been proposed, the lack of prior reports demonstrating that thyroid hormones and thyromimetics can reduce serum cholesterol in the absence of LDLRs has led to the inference that cholesterol reduction by TR agonists is primarily an LDLR-dependent effect. Results of the current study reveal this assumption to be incorrect and demonstrate that TR activation can reduce serum cholesterol via an LDLR-independent mechanism.

Of the potential LDLR-independent mechanisms of cholesterol reduction by TR activation, the most commonly proposed is induction of the HDL receptor, SR-BI, leading to an increased rate of reverse cholesterol transport (*40*). While several reports have indicated that thyroid hormones can stimulate SR-BI expression, we do not believe that this effect plays an important role in cholesterol reduction in

LDLR$^{-/-}$ mice. First, we did not observe changes in SR-BI expression, at either the transcript or protein level, in LDLR$^{-/-}$ or C57 mice. Secondly, cholesterol reduction in LDLR$^{-/-}$ mice is largely restricted to the LDL fraction and there is little change in HDL cholesterol following thyromimetic treatment. Finally, while SR-BI induction and increased reverse cholesterol transport appears a quite reasonable mechanism by which thyroid hormones could reduce cholesterol in most rodent species, which maintain the majority of their serum cholesterol as HDL cholesterol, it is difficult to rationalize how such a large decrease in LDL cholesterol levels could result from this mechanism in LDLR$^{-/-}$ mice, for which nearly all serum cholesterol is carried via LDL particles and have limited ability to transfer cholesterol between LDL and HDL particles due to their lack of cholesteryl ester transferase protein activity.

Instead, our results suggest that the TR agonists tested here reduce serum cholesterol levels in LDLR$^{-/-}$ mice by strongly inducing Cyp7a1, resulting in increased cholesterol to bile acid conversion and increased fecal bile acid excretion. That similar effects on Cyp7a1 expression and bile acid synthesis were observed in wild-type C57 mice, in the absence of LDLR or SR-BI induction, suggest to us that the reductions in serum cholesterol brought about by thyroid hormones and TR activation may be mediated primarily via the induction of Cyp7a1. Indeed, the effects elicited by TR activation correspond nearly wholly with those seen in mice following hepatic overexpression of

Cyp7a1. Increased Cyp7a1 activity has been demonstrated to be sufficient to lower plasma cholesterol levels in $LDLR^{-/-}$ mice and WHHL rabbits, both of which lack functional LDLRs (*99*–*101*). In accordance with our findings, this action did not require the induction of alternative hepatic lipoprotein receptors or hepatic cholesterol efflux transporters (*100*). The TR agonists studied did not reduce hepatic cholesterol levels despite strongly increasing hepatic excretion of bile acids. This is presumably due to increase/;d hepatic synthesis of cholesterol, since Cyp7a1 overexpression has been shown to evoke a compensatory increase in *de novo* cholesterol synthesis, preventing a decrease in hepatic cholesterol (*101*, *102*) and T_3 treatment has been shown to have similar effects on hepatic cholesterol synthesis (*103*).

The mechanism by which Cyp7a1 induction affects plasma lipoproteins appears to be multivariate and is not well understood. Consistent with Cyp7a1 being the primary mediator behind the lipid lowering actions of TR activation, the manner by which the TR agonists tested reduce serum cholesterol and triglycerides appears to be correspondingly complex. Similar to prior reports, which have shown that T_3 and Cyp7a1 overexpression increase hepatic triglyceride and VLDL secretion (*96*–*98*, *104*), GC-1 treatment elicited an increase in the secretion of triglycerides and ApoB despite markedly decreasing total serum triglyceride and LDL cholesterol levels. This paradoxical effect of hepatic Cyp7a1 activation may help explain the divergent reports relating TR agonist treatment

with serum triglyceride levels (*38*, *40*, *88*). Indeed, we have found that, in contrast to the results presented here, the treatment of non-hypertriglyceridemic mice with thyromimetics increases serum triglyceride levels.

As Cyp7a1 has been shown previously to be a TR regulated gene in mice (*105*) and rats (*106*), it is perhaps not surprising that these compounds increased Cyp7a1 expression. However, the magnitude of the cholesterol reduction brought about by Cyp7a1 induction was quite unanticipated in light of the fact that the aforementioned studies demonstrating the ability of Cyp7a1 induction to reduce serum cholesterol utilized transgenic and viral over-expression methods. Thyromimetics could represent a novel avenue for treatment of defects in cholesterol metabolism associated with hFH. In accordance with animal studies, where Cyp7a1 overexpression leads to reduced serum cholesterol and triglycerides and increased bile acid excretion, human deficiency in Cyp7a1 results in elevated serum cholesterol and triglycerides and an appreciably reduced rate of bile acid excretion (*107*) suggesting that increasing Cyp7a1 expression may be a viable LDLR-independent pharmacological strategy to reduce serum cholesterol in man. The regulation of Cyp7a1 has been reported to differ between rodents and humans (*108*), implying that these results may not translate to clinical studies. However, similar to our findings here, KB2115 has been shown to strongly stimulate bile acid synthesis in humans (*109*), increasing serum C4 levels by over 100%, indicating that a similar mechanism may play a

role in the cholesterol lowering effects of TR activation in man. This potential ability to reduce cholesterol via a mechanism distinct from the statin drugs may also provide a rationale behind the clinical efficacy of KB2115, which has been shown to act additively when administered concurrently with statins, further reducing total and LDL cholesterol levels when given to hypercholesterolemic patients already being treated with statins (*110*).

In conclusion, the thyroid hormone T_3 and the thyromimetics GC-1 and KB2115 reduce serum cholesterol via an LDLR-independent mechanism that appears to be mediated primarily by the induction of Cyp7a1 and increased bile acid synthesis, making it distinct from that of most other cholesterol lowering therapies. This class of compounds may have value in treating high cholesterol, especially for diseases such as hFH, for which LDLR induction is minimally effective. Given the lack of effective treatment options for affected hFH patients and the severity of the disease, thyromimetics such as GC-1 and KB2115 may warrant evaluation for their ability to lower serum cholesterol in this population.

Materials and Methods

Animals

Male $LDLR^{-/-}$ and C57 mice were obtained from Jackson Labs (Maine) and housed in a temperature-controlled environment with 12 h light/dark cycles and

fed standard irradiated rodent chow *ad libitum* (TD.2918, Harlan Teklad). All mice used in the studies were male aged-matched of 4 months of age. Prior to treatment mice were fed a western diet containing 0.2% cholesterol (D12079B, Research Diets) for 12 weeks. Unless otherwise noted, at 6 week-old mice were fed a western diet containing 0.2% cholesterol (D12079B, Research Diets) for 12 weeks. All animal experiments were approved by the Methodist Hospital Research Institute Institutional Animal Care and Use Committee.

Animal Treatments

Triiodothyronine (T2877; Sigma), KB2115 (10011054; Cayman), and atorvastatin (sc-337542; Santa Cruz Biotechnology) dissolved in DMSO were administered by intraperitoneal injection. GC-1 was administered by either intraperitoneal injection or admixed in the diet (western diet, Research Diets) and provided *ad libitum*. Details of each experiment are described in figure legends. In all cases, animals in the control group received the appropriate vehicle solutions and diets identical to the treatment groups.

Lipid And Lipoprotein Analysis

For hepatic lipid analysis, liver tissue was homogenized and total lipids were extracted from liver using a Folch solution (chloroform/methanol, 2:1), precipitated with sodium chloride, dried and resuspended in 2% Triton X-100 PBS. Plasma and tissue lipid extracts were assayed for cholesterol and

triglycerides using commercial kits (Thermo Scientific). For lipoprotein profiling pooled plasma was separated by FPLC using two Superose 6 columns (GE Healthcare) linked in tandem, 300 ml fractions were collected and lipid levels were analyzed in each fraction using a fluorescence enzymatic assay (Cayman).

Plasma C4 (7α-hydroxy-4-cholesten-3-one) Levels

Plasma 7α-hydroxy-4-cholesten-3-one levels were measures as described (*88*) with modifications. Deuterium labeled C4 (Santa Cruz Biotechnology) internal standard was added to 10 µl of plasma, followed by ammonium sulfate and acetonitrile precipitation, supernatant was dried and resuspended in methanol. Plasma C4 levels were measured using LC-ESI-MS/MS (*111*) on an Acquity® UPLC system (Waters Corp) and XevoTQ® mass spectrometer (Waters Corp) operated in the MRM mode using positive ion electrospray conditions. C4 levels were normalized to total cholesterol levels.

Fecal Sterol Analysis

Mice were acclimated to metabolic cages prior to a 72-hour feces collection. Dried feces were boiled in alkaline methanol (1 M NaOH/Methanol, 1:3) after addition of 5α-cholestane as an internal standard for neutral sterol analysis. After cooling to room temperature, neutral sterols were extracted using petroleum ether, the combined organic layers was dried and redissolved in hexane for gas

chromatography analysis. Total bile acids in the aqueous layer were measured using a spectrophotometric enzymatic assay (Diazyme).

Immunoblotting

Liver tissue was homogenized in tissue extraction reagent (Invitrogen) containing complete protease inhibitor (Roche Diagnostics). Equivalent amounts of total protein were separated by SDS-PAGE, transferred to polyvinylidene difluoride membranes and probed with anti-SR-BI (ab3), anti-LDLR (ab52818) or anti-β-actin (6267) antibody (Abcam) and secondary conjugated-HRP anti-rabbit or (sc-2004) anti-mouse (sc-2005) antibody (Santa Cruz Biotechnology). The proteins were visualized using Amersham ECL Western Blotting Detection Regents (GE Healthcare) and autoradiography.

RNA Extraction and Real-time qPCR

Total RNA was extracted and isolated using Qiazol and RNeasy Mini Kit according to manufacturer's protocol (Qiagen). First strand cDNA was transcribed from 2.5 mg of total RNA using SuperScript VILO cDNA Synthesis Kit (Invitrogen). TaqMan real-time PCR reactions were performed on a LightCycler 480 Real-Time PCR system (Roche) and relative mRNA levels were calculated by comparative C_t method using β-actin as the internal control. TaqMan primer/probe sets supplied by Applied Biosystems were used (Assay IDs are available upon request).

Hepatic Triglyceride and ApoB Secretion Rate Determination

Triglyceride and apoB secretion rate was performed as previously described (*112*). Mice fasted for 4 h were injected with poloxamer 407 (1000 mg/kg) and 200 μCi of [^{35}S]-methionine. Blood samples were collected prior to injection and at 60 and 120 min following. The concentration of serum triglycerides was measured using commercial kits. For ApoB secretion rate, plasma samples were separated on a 3-8% SDS-PAGE gel. The gel was dried under vacuum and exposed to x-ray film. Bands representing newly synthesized [^{35}S]-labeled ApoB were excised and counted via liquid scintillation.

Statistical Analysis

All results are expressed as mean ± SEM. Statistical analysis was performed using GraphPad Prism software. Comparisons of groups were performed using Student's T-test. A *p*-value of less than 0.05 was considered significant.

CHAPTER 3 THYROID HORMONE RECEPTOR AGONISTS ELICIT A FUNCTIONAL CONVERSION OF WHITE TO BROWN FAT

Functional conversion of white adipose tissue (WAT) into a tissue with brown adipose tissue (BAT)-like activity may be an important strategy to combat obesity and control type 2 diabetes. We demonstrate that thyroid hormone receptor (TR) activation by T_3 or the synthetic agonist GC-1 induces a program of adaptive thermogenesis and uncoupled respiration in subcutaneous WAT that is correspondent with the amelioration of obesity and insulin resistance. Surgical denervation of BAT has no effect on systemic thermogenesis, and all thermogenesis is lost in lean mice that possess little subcutaneous WAT, suggesting that induction of thermogenesis is mediated by WAT. These data demonstrate that TR activation can elicit facultative thermogenesis in WAT, a previously unrecognized component of TR-mediated thermogenesis, and establish the profound pharmacological potential of WAT browning.

INTRODUCTION

Obesity is an accelerating worldwide health crisis associated with co-morbidities that include diabetes, hyperlipidemia, and hypertension. The World Health Organization estimates that over 500 million adults worldwide are obese and attributes 2.8 million annual deaths to obesity associated disease (*113*). Obesity is caused by a chronic imbalance of excess caloric intake relative to expenditure (*114*, *115*). The excess energy, which is stored as lipid within white fat, leads to an expansion of this tissue. While nearly everyone is familiar with

WAT, typically referred to simply as ‘fat’, there is far less appreciation for BAT, a unique type of adipose tissue. By uncoupling oxidative metabolism from ATP generation, BAT has the relatively unique capacity to perform adaptive thermogenesis, the conversion of excess energy to heat. This ability gives BAT high metabolic potential; when activated, BAT can double metabolic rate in rodents (*116*). Thus, while WAT serves primarily to store excess energy, BAT can dispose of excess energy by converting it to heat (*53*, *117*).

Since BAT-mediated adaptive thermogenesis is inherently anti-obesogenic (*66*, *67*), there has long been an interest in harnessing this action to treat obesity (*118*). However, until recently, it was generally accepted that adult humans did not possess brown fat (*53*, *115*) implying that the direct targeting of BAT was not a viable therapeutic approach. Instead, it was questioned whether WAT could be induced to become more BAT-like (*119*), thus increasing energy expenditure. The prospect of doing so was bolstered by evidence of BAT-like, or 'beige' cells appearing within WAT depots in response to cold exposure or treatment with β-adrenergic agonists (*77*, *79*, *120*). Although tantalizing, the physiological relevance of these beige cells was unclear and it was not apparent how to harness this effect clinically (*121*).

Two recent events have led to a strong renewed interest in utilizing adaptive thermogenesis to combat obesity. First, several groups have reported the

existence of active brown fat in adult humans (*68*–*72*). Furthermore, BAT activity in humans appears to correlate with resistance to obesity (*69*, *70*). Second, numerous reports in the past year have demonstrated the ability to impart BAT-like function within WAT depots of rodents, a process often referred to as 'browning' (*21*–*24*). While these examples have shown that the induction of BAT-like adaptive thermogenesis in WAT can have anti-obesogenic and anti-diabetic effects, the magnitude of these effects have generally been modest despite the use of genetically engineered mice, leading some to question the pharmacological potential of browning (*122*).

It is well established that TR signaling is involved in the regulation of thermogenesis, body temperature (*42*), and energy balance (*32*). In humans, hypothyroidism is associated with hypersensitivity to cold while hyperthyroid individuals have difficulty tolerating heat (*18*). Loss of TR signaling in rodents, either by ablation of TRs or by thyroidectomy, results in decreased body temperature and cold intolerance (*10*, *123*). Although TR-mediated thermogenesis is generally attributed to BAT, the relationship between TR activation and thermogenesis is complex and has not been fully resolved (*42*). Here we report that TR activation by the synthetic agonist GC-1 and the endogenous ligand T_3 elicits a BAT-like program of adaptive thermogenesis and uncoupled respiration in subcutaneous WAT (scWAT). This action, which is accompanied by marked increase in metabolism and dramatic fat loss, appears

to be mediated principally by WAT, suggesting that the browning of WAT may represent an unappreciated component of TR-induced thermogenesis.

RESULTS

The TR Agonist GC-1 Elicits a BAT-like Program of Adaptive Thermogenesis in scWAT

To explore how TR agonists induce thermogenesis *in vivo*, we treated genetically obese (ob/ob) mice with the synthetic agonist GC-1 and profiled changes in the expression of markers of thermogenesis and uncoupled respiration (*Ucp1*, *Ppargc1a*, *Prdm16*, *Elovl3*, *Cidea*, *Pparg*, *Cebpb*, and *Dio2*) (*53*, *73*, *124–126*) and mitochondrial function (*Tfam*, *Nrf1*, *Cycs*, *Cox4*) (*114*, *126*) in BAT, epididymal WAT, and scWAT depots (Figure 3-1 A-D). A similar panel of markers, including genes involved in oxidative metabolism or previously implicated in muscle-mediated thermogenesis (*Serca1* and *Serca2*, *Ucp3*, *Cpt1a* and *Cpt1b*, *Mcad*, *PDK4*, *Myh7*, *Myh1*, and *Myh4*) (*127*), was used to monitor changes in muscle gene expression (Figure 3-1D). Somewhat surprisingly, GC-1 significantly repressed all markers in BAT (Figure 3-1A). In contrast, the expression of all genes was strongly induced in scWAT, with levels of *Ppargc1a*, *Elovl3*, *Cidea*, *Dio2*, *Cox5a*, and *Cebpb* increased by over 10-fold, while Ucp1 levels were increased by over 100-fold (Figure 3-1B). Estimation of absolute transcript levels suggested that, following GC-1 treatment, *Ucp1* mRNA levels in

scWAT were similar to those found in BAT (Figure 3-2). In epididymal WAT, *Ucp1* levels were increased, although expression of other genes in the thermogenic program were either decreased or unchanged (Figure 3-1C). GC-1 altered expression levels of *Serca2*, *Ppargc1a*, *Cox5a*, and *Myh4* in muscle, although expression of other genes including *Ucp1* was unchanged and the magnitude of the observed changes was small relative to the alterations seen in

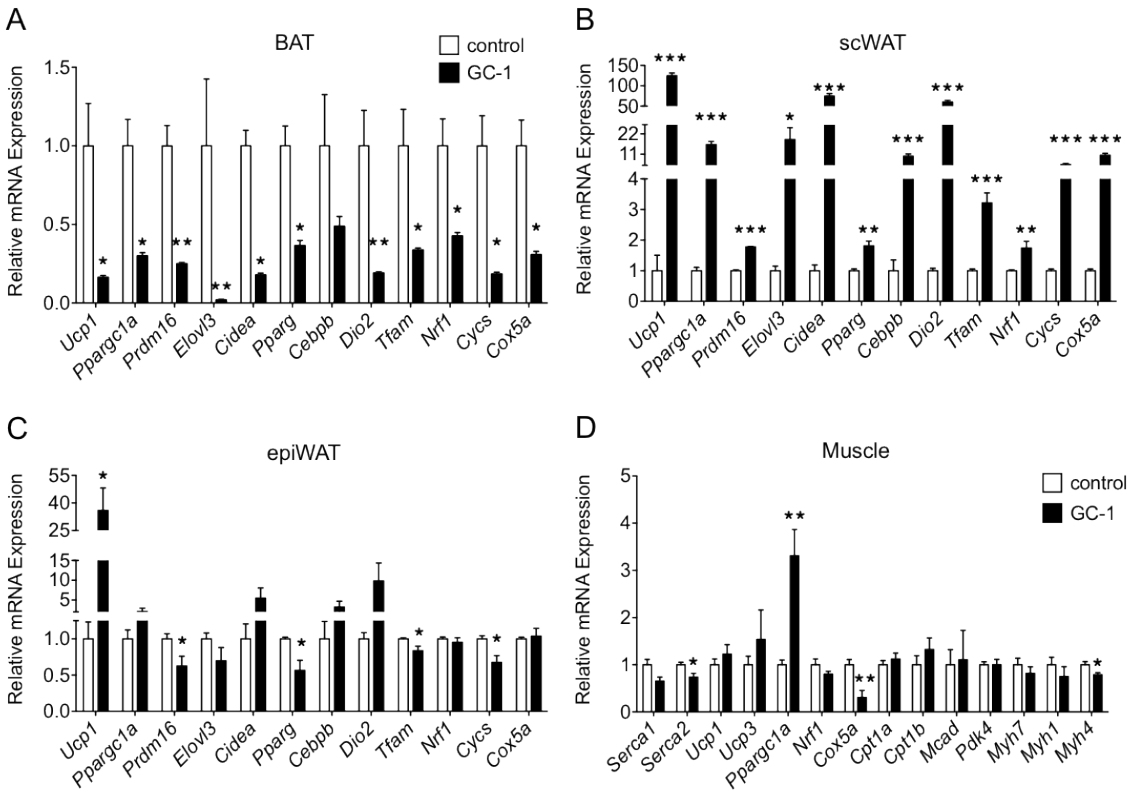

Figure 3-1. Thermogenic gene expression in BAT, scWAT, epiWAT and muscle.
Male ob/ob mice were fed standard chow with or without admixed GC-1 for 21 days (n = 4–6). At the end of day 21, mice were sacrificed and tissues were collected. Thermogenic gene expression was measured in brown adipose tissue (BAT) (A), subcutaneous white adipose tissue (scWAT) (B), epididymal white adipose tissue (epiWAT) (C) and gastrocnemius muscle (d) of GC-1 treated and untreated mice. Data are mean ± s.e.m. *P < 0.05, **P < 0.01, ***P < 0.001.

scWAT and BAT (Figure 3-1D). These data suggest that the TR agonist GC-1 induces the full genetic program of thermogenesis and uncoupled respiration in scWAT.

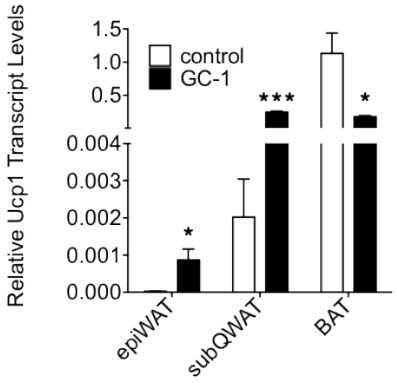

Figure 3-2. Similar levels of *Ucp1* transcript in scWAT of GC-1 as BAT.
Relative *Ucp1* transcript levels in epiWAT, subQWAT, and BAT (n = 4–6). Data are mean ± s.e.m. *P < 0.05, ***P < 0.001.

Since UCP1 is generally considered the key mediator of uncoupled respiration in adipocytes, we investigated how GC-1 affected UCP1 protein levels within the various adipose tissue depots. While UCP1 protein levels were unaltered in BAT, the effect in scWAT was striking. UCP1 protein, which was undetectable in the scWAT of untreated mice, was increased at least 100-fold, reaching a level equivalent to 40% of that found in BAT (Figure 3-3). UCP1 levels were undetectable in epididymal WAT of both treated and untreated animals.

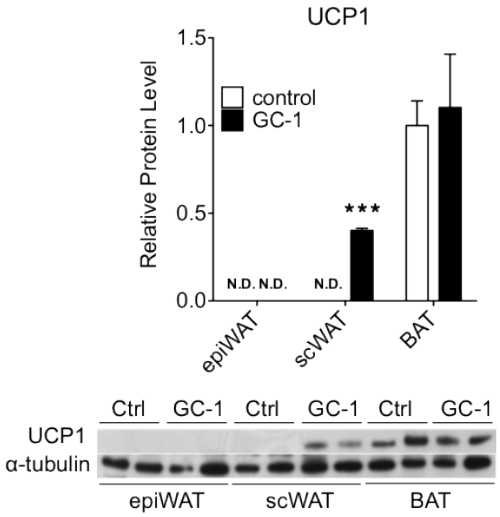

Figure 3-3. GC-1 induces an increase in UCP1 protein in scWAT.
UCP1 protein expression in epiWAT, scWAT, and BAT of GC-1 treated and untreated mice (n = 4–6). Data are mean ± s.e.m. ***P < 0.001. N.D., not detectable.

Histological examination of adipose tissue depots revealed striking morphological changes in the scWAT of GC-1-treated mice (Figure 3-4). Subcutaneous white adipocytes of treated mice were smaller and approximately 40% of the cells

acquired multilocular lipid droplets, both features common to brown adipocytes (*77*, *128*). Conversely, adipocytes from the BAT depot of treated mice were larger with decreased multilocularity. Adipocytes of epididymal WAT exhibited little morphological change. To further investigate changes in the metabolic

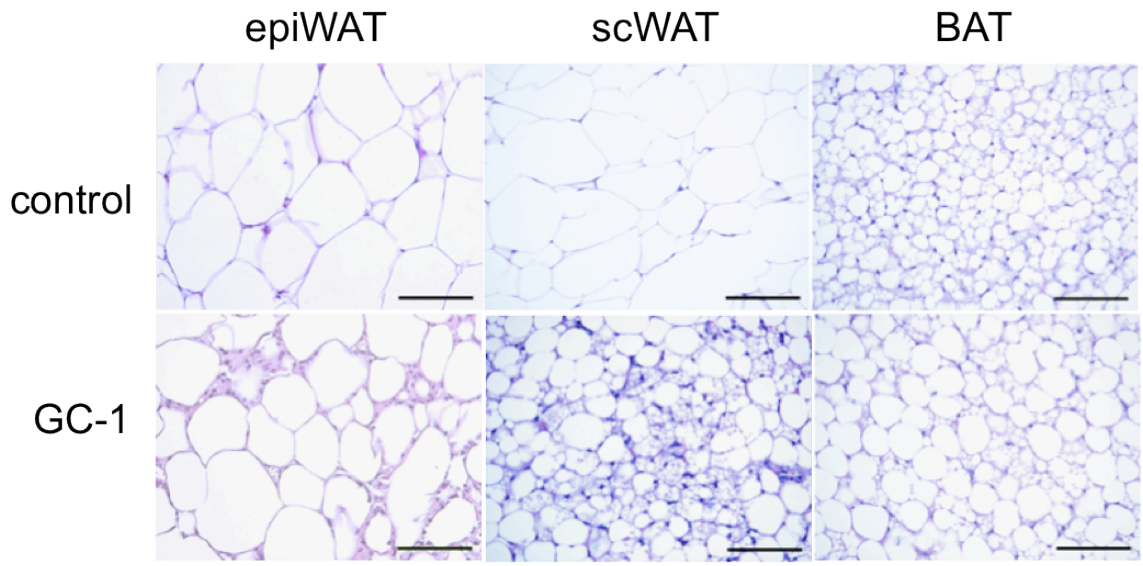

Figure 3-4. GC-1 induces mutlilocular lipid droplets in scWAT.
Representative images of epiWAT, scWAT, and BAT were stained with H&E. Scale bar, 100 μm.

parameters of various adipose tissue depots, we measured mitochondrial DNA content (Figure 3-5A) and citrate synthase activity as well as the respiration rate of scWAT (Figure 3-5C). Following GC-1 treatment, mitochondrial DNA and citrate synthase increased substantially in scWAT (Figure 3-5B). No changes were observed in epididymal WAT or BAT. Basal respiration was doubled in scWAT of GC-1-treated mice (Figure 3-5C). Since SNS stimulation is required for activation of the adaptive thermogenic program, we measured norepinephrine levels in BAT and scWAT. Norepinephrine levels, which were substantially decreased in BAT of GC-1-treated mice, increased by 48% in scWAT (Figure 3-

5D). Collectively, GC-1 induces genes involved in adaptive thermogenesis, induces mitochondrial biogenesis, increases UCP1 protein, increases metabolic rate, and elicits morphological changes in scWAT that are consistent with a BAT-like phenotype, indicating that GC-1 imparts brown fat-like function to scWAT.

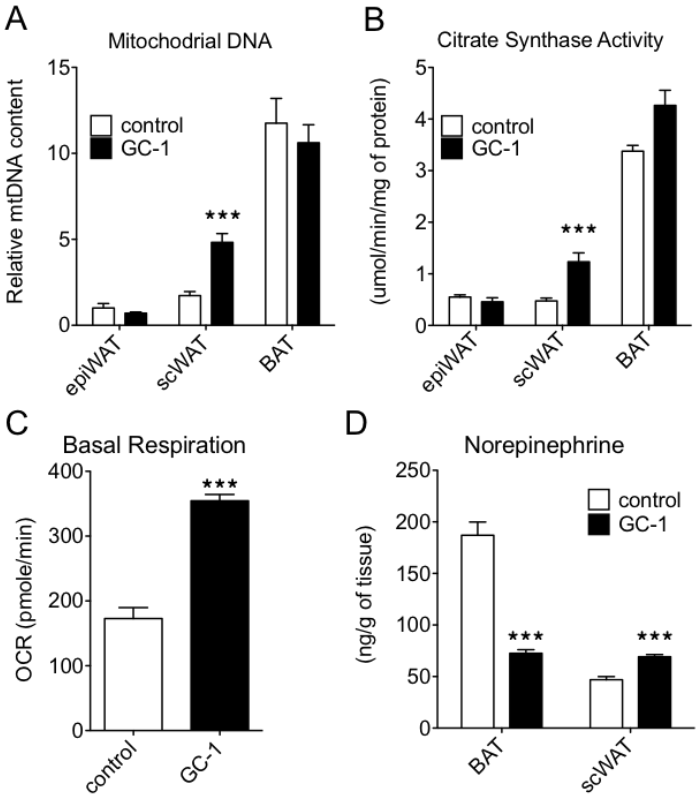

Figure 3-5. GC-1 induces increase in mitochondria and respiration in scWAT.
Mitochondrial DNA content (A) and citrate synthase activity (B) were measured in epiWAT, scWAT, and BAT. (C) Oxygen consumption rate in scWAT of GC-1 treated and untreated mice. (D) Norepinephrine content in BAT and scWAT of GC-1 treated and control mice. Data are mean ± s.e.m, n = 4–6. ***P < 0.001.

GC-1-induced Browning of scWAT Coincides with Marked Thermogenesis and Metabolic Elevation

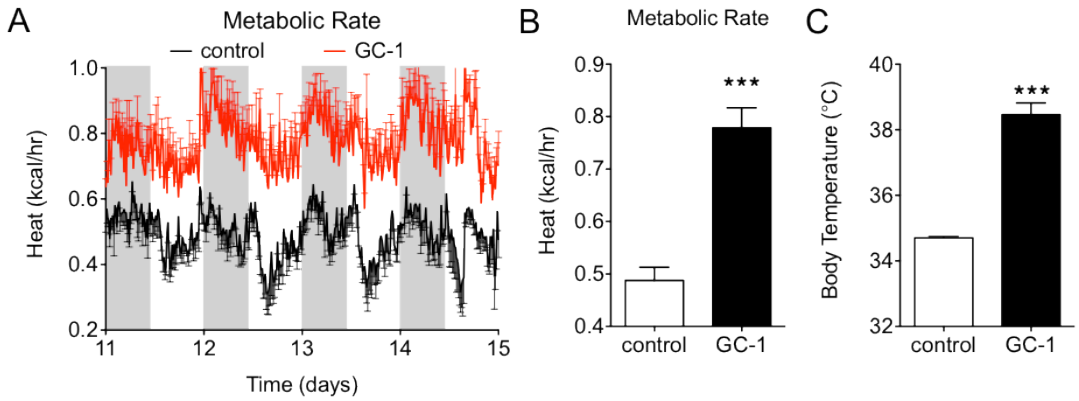

Figure 3-6. GC-1 induces an increase in metabolic rate and body temperature.
Male ob/ob mice fed diets with or without GC-1 were monitored in metabolic cages (n = 4). Metabolic rates were measured by indirect calorimetry at 15 min intervals (A) and the average metabolic rate was assessed over a 72-h period (b). Body temperature was measured after 21 days of treatment (n = 4). Data are mean ± s.e.m. ***P < 0.001.

Several recent reports have demonstrated the capacity to induce a program of brown fat-like thermogenesis in WAT (*73*–*76*). These reports have almost universally suggested that the observed WAT-mediated thermogenesis was sufficient to elicit anti-obesity and anti-diabetic actions (*73*, *75*, *129*). To examine metabolic effects that coincided with the induction of brown-fat-like function in WAT, we monitored body temperature and used indirect calorimetry to measure changes in metabolic rate that accompanied GC-1 treatment. GC-1 treatment was found to raise mean metabolic rate by nearly 60% (Figure 3-6, A and B), and increased body temperature by 3.8°C (Figure 3-6C), an increase large enough to

be readily apparent while handling the animals. The induction of thermogenesis

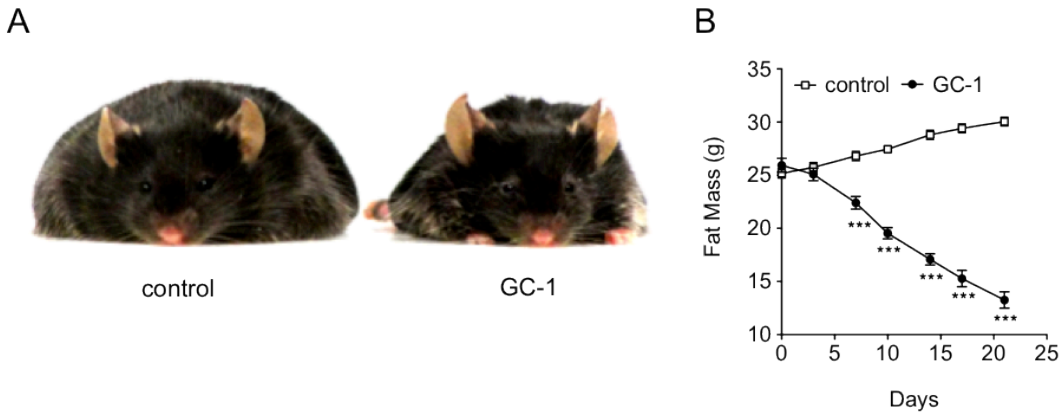

Figure 3-7. Dramatic weight and fat loss in ob/ob mice treated with GC-1.
(A) Representative images were taken of GC-1 treated (right) and untreated (left) mice after 21 days of GC-1. (B) Body fat monitored over the duration of treatment (n = 4). Data are mean ± s.e.m. ***P < 0.001.

was accompanied by marked weight and fat loss (Figure 3-7, A and B**).** GC-1 treatment did not alter food intake and treated mice were less active than untreated controls, indicating that weight loss resulted solely from increased metabolic rate (Figure 3-8, A and B). Lean mass was found to increase following

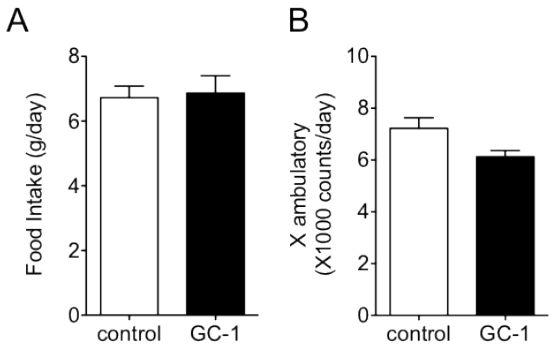

Figure 3-8. No change in food intake or physical activity.
Food intake (A) and ambulatory activity (B) were assessed and averaged over a 3-day period (n = 4). Data are mean ± s.e.m.

GC-1 treatment (Figure 3-9A), indicating that weight loss was due exclusively to a loss of adiposity. GC-1 treatment also led to a rapid and substantial decrease

in the respiratory exchange ratio (RER), with values approaching the theoretical minimum of 0.7 (Figure 3-9B), indicating that GC-1 treatment elicited a significant shift from the utilization of carbohydrates to fatty acids as substrate in oxidative metabolism. The change in RER is consistent with reports demonstrating that uncoupling of oxidative phosphorylation by either chemical uncouplers (*130*) or non-shivering adaptive thermogenesis (*131*) increases the oxidation of fatty acids relative to carbohydrates.

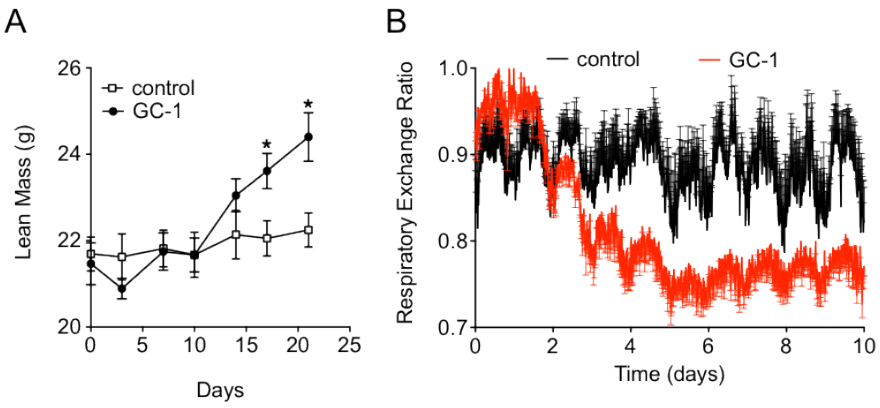

Figure 3-9. Weight loss is due solely to loss of adiposity.
(A) Lean mass was monitored in treated and untreated mice over the duration of treatment. (B) Respiration exchange ratio was measured from the ratio of V(CO2) produced to V(O2) consumed (n = 4). Data are mean ± s.e.m. *P < 0.05.

Leptin-deficient mice are hypothermic due to defects in adaptive thermogenesis, resulting in depressed body temperature and intolerance to cold (*132*). Since GC-1 treatment normalized the body temperature of ob/ob mice (Figure 3-10), we questioned whether GC-1-induced thermogenesis could also restore cold

tolerance to these mice. Untreated mice exhibited pronounced shivering and piloerection (i.e. goosebumps), both expected physiological responses, almost immediately upon exposure to 4°C. Additionally, the body temperature of untreated animals was found to decrease sharply when challenged with cold (Figure 3-10). Conversely, GC-1-treated animals experienced no decrease in body temperature after 15 hours at 4°C. Remarkably, treated animals exhibited no apparent shivering or piloerection, suggesting that the program of adaptive thermogenesis elicited by GC-1 obviated the need for shivering, generally a key component of heat generation in response to cold (*133*).

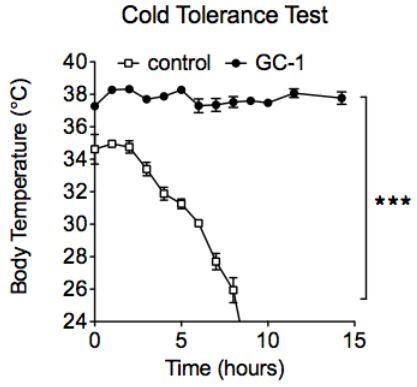

Figure 3-10. GC-1 rescues thermogenic effect of ob/ob mice.
Body temperature was measured during a cold tolerance test after 21 days of GC-1 treatment (*n* = 4). Data are mean ± s.e.m. ****P* < 0.001.

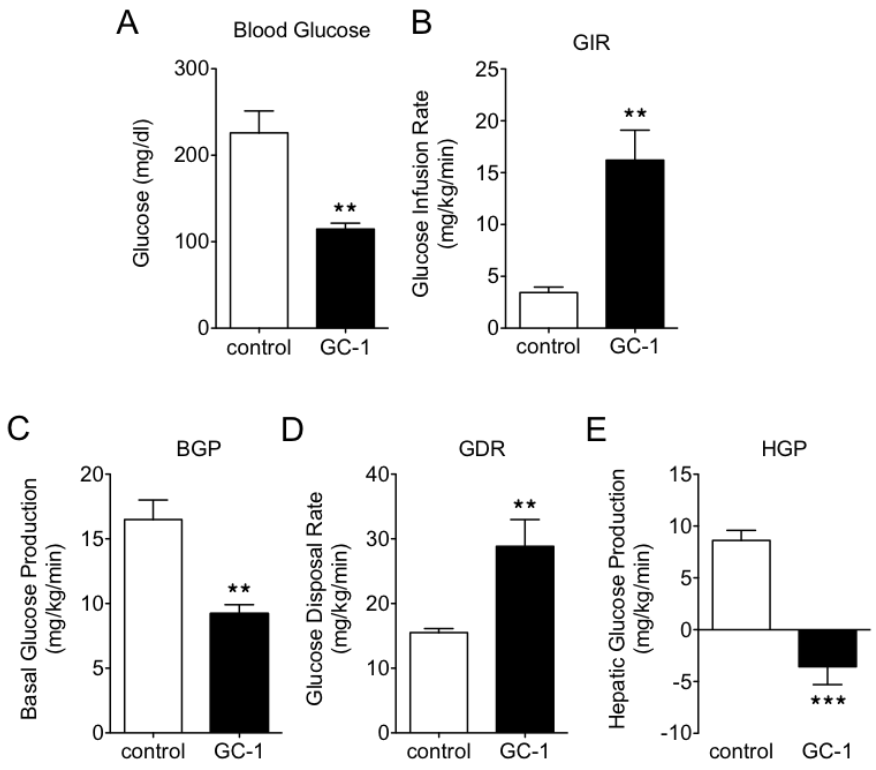

Figure 3-11. Improved insulin sensitivity assessed by hyperinsulinemic-euglycemic clamp. Fasting blood glucose (A) and glucose infusion rate (B) were measured during a hyperinsulinemic-euglycemic clamp experiment on days 10-12 of treatment (n = 6). (C) Basal glucose production rate was discerned from blood samples collected prior to insulin infusion. Glucose disposal rate (D), and hepatic glucose production rate (E) were during hyperinsulinemic-euglycemic clamp for GC-1-treated and control mice. Data are mean ± s.e.m. $^{**}P < 0.01$, $^{***}P < 0.001$.

To determine whether GC-1-induced adaptive thermogenesis affected insulin sensitivity and glycemic control, we conducted a hyperinsulinemic-euglycemic clamps study as well as a glucose tolerance test. GC-1 treatment normalized fasting glucose levels, notably increased glucose infusion rate, and led to improvements in basal glucose production, glucose disposal rate, and hepatic glucose disposal (Figure 3-11, A-E); all indicative of substantially increased insulin sensitivity. GC-1-treated mice also exhibited markedly improved glycemic

control (Figure 3-12, A and B). Thus, the metabolic effects of GC-1 include marked anti-diabetic actions. Collectively, these results suggest that TR activation by GC-1 strongly induces a program of non-shivering adaptive thermogenesis which results in metabolic increase that ameliorates obesity and insulin resistance and is sufficient to compensate fully for thermogenic defects inherent to ob/ob mice.

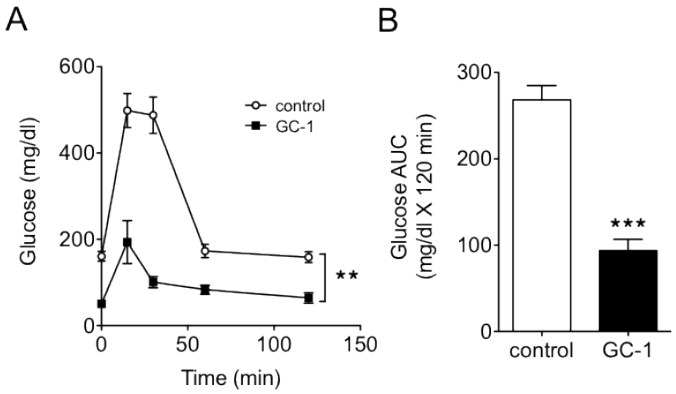

Figure 3-12. Increases glucose tolerance of control and GC-1 treated ob/ob mice.
Glucose tolerance test (A) and area under the curve quantification (B) of treated and untreated ob/ob mice was assessed at day 21 (n = 5–6). Data are mean ± s.e.m. $^{**}P < 0.01$, $^{***}P < 0.001$.

GC-1 Mediated Adaptive Thermogenesis is Independent of BAT Activity

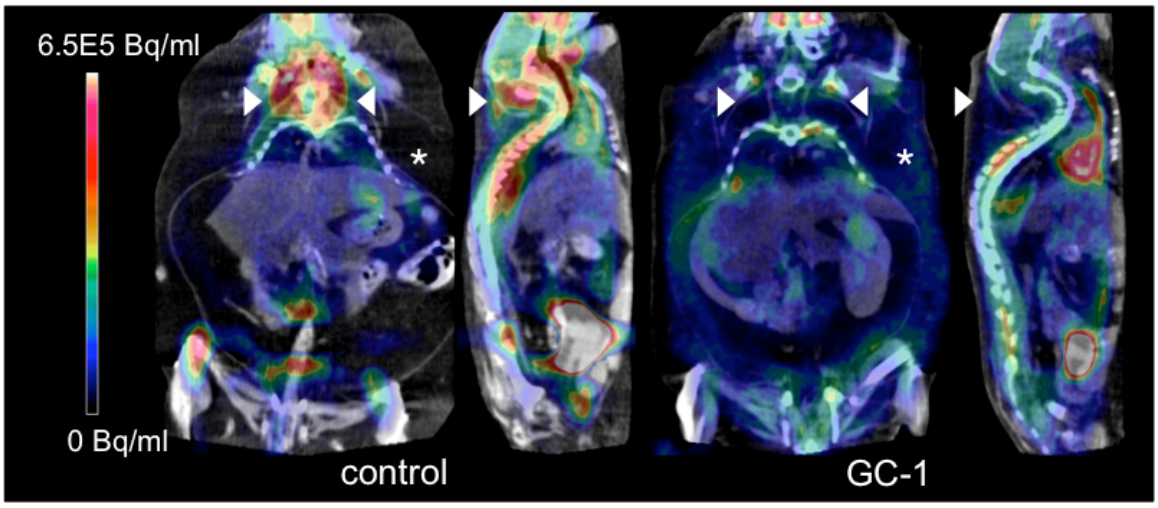

Figure 3-13. 18F-FDG PET/CT imaging of control and GC-1 treated ob/ob mice.
Representative PET-CT image of 18F-FDG uptake in BAT (arrowheads) and scWAT (*) in untreated (left) and treated (right) ob/ob mice.

Given the magnitude of GC-1-induced thermogenesis and the fact that thyroid hormone associated thermogenesis is generally attributed to BAT (*42*, *134*) we felt that it was important to further explore whether BAT contributed to the thermogenic actions of GC-1. We used PET/CT imaging to examine the effects of GC-1 treatment on glucose metabolism in BAT and other peripheral tissues of mice placed under a mild cold stress (19-20°C). In untreated mice, ^{18}F-FDG (FDG) uptake in interscapular BAT was readily apparent (Figure 3-13). Following GC-1 treatment, however, FDG uptake in interscapular BAT became indistinguishable from uptake in surrounding tissue, suggesting that GC-1 strongly decreases the metabolic activity of interscapular BAT. Instead, GC-1 treated mice exhibited diffuse FDG uptake into extra-abdominal regions

corresponding to scWAT. FDG uptake into equivalent regions of untreated mice was not detectable. Similar changes in glucose metabolism were observed during the hyperinsulinemic-euglycemic clamp study. Under hyperinsulinemic

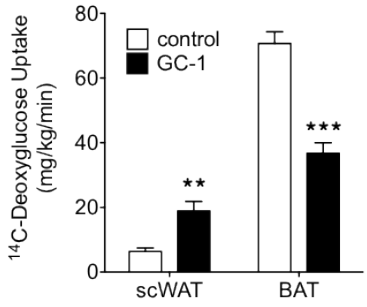

Figure 3-14. Glucose uptake in scWAT and BAT of control and treated ob/ob mice.
14C-deoxyglucose uptake in scWAT and BAT of treated and untreated mice measured during a hyperinsulinemic-euglycemic clamp experiment (*n* = 6). Data are mean ± s.e.m. ***P* < 0.01, ****P* < 0.001.

conditions, ^{14}C-deoxyglucose uptake into scWAT increased significantly in GC-1 treated mice, while glucose uptake into BAT was decreased (Figure 3-14). To more firmly establish that BAT did not contribute to TR-mediated thermogenesis,

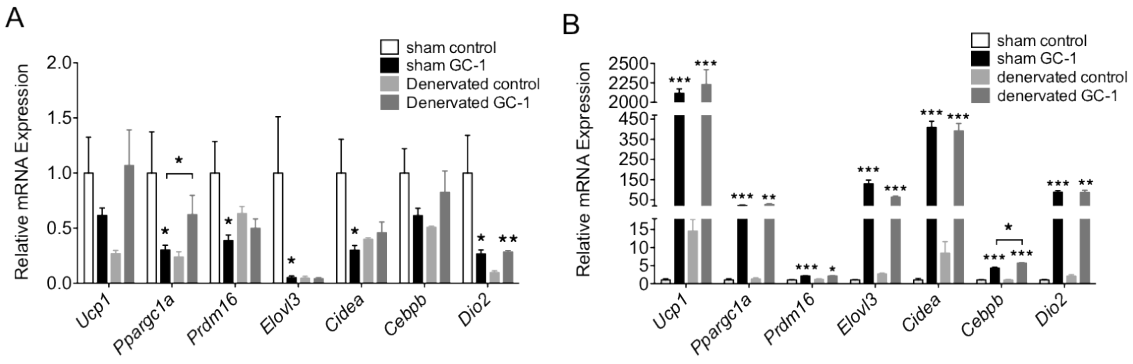

Figure 3-15. Thermogenic gene expression in scWAT and BAT of sham and BAT-denervated ob/ob mice.
Thermogenic gene expression in BAT (A) and scWAT (B) of BAT-denervated and sham mice treated with or without GC-1 supplementation for 21 days (*n* = 6 per sham group; n = 3 per BAT denervated group). Data are mean ± s.e.m. **P* < 0.05, ***P* < 0.01, ****P* < 0.001.

GC-1 was administered to mice in which intrascapular BAT activity had been ablated by surgical denervation (Figure 3-15A). While denervation reduced the expression of thermogenic markers in BAT, GC-1 treatment induced thermogenic gene expression in scWAT (Figure 3-15B) and resulted in weight (Figure 3-16A) and fat loss (Figure 3-16B) and elevation of body temperature (Figure 3-16C) that was indistinguishable between BAT-denervated mice and sham-treated controls, indicating that interscapular BAT does not make a measurable contribution to the metabolic effects elicited by GC-1.

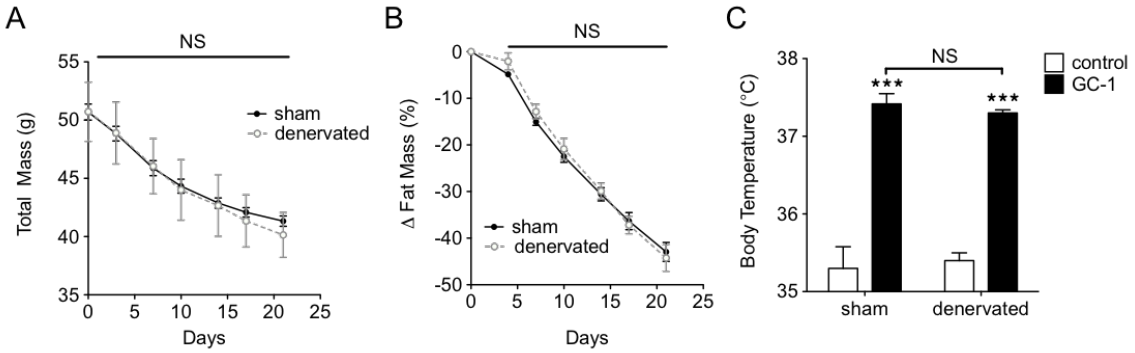

Figure 3-16. Indistinguishable weight and fat loss and elevated body temperature between BAT-denervated and sham treated mice.
Weight loss (A), change in fat mass (B) and body temperature (C) were measured in BAT-denervated and sham mice (n = 6 per sham group; n = 3 per BAT denervated group). Data are mean ± s.e.m. *P < 0.05, **P < 0.01, ***P < 0.001. NS, not significant.

In Addition To GC-1, T_3 Also Induces Adaptive Thermogenesis in scWAT of ob/ob Mice

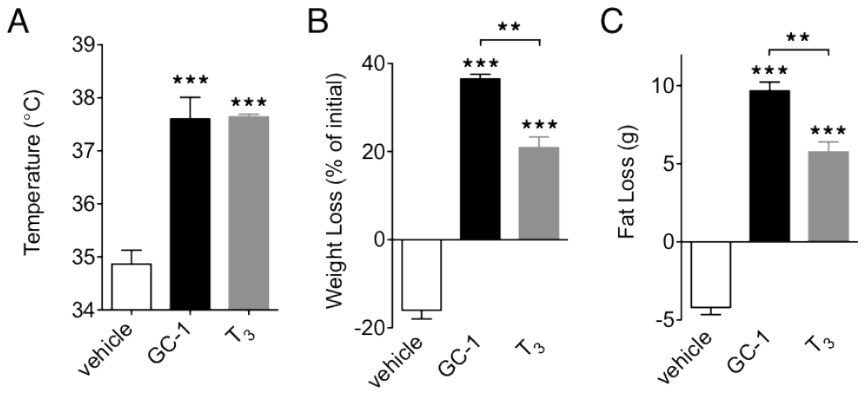

Figure 3-17. T_3 treatment induces similar weight and fat loss and increases body temperature.
Male ob/ob mice were administered GC-1, T3 or vehicle via daily intraperitoneal injections for 14 days (*n* = 4). Body temperature (A), weight loss (B) and fat loss (C) of mice after 14 days of GC-1, T3 or vehicle treatment. ***P* < 0.01, ****P* < 0.001.

To assess whether the phenomenon of WAT browning was unique to the agonist GC-1 or whether T_3 could induce similar effects, we treated ob/ob mice with either GC-1 or pharmacological doses of T_3. Both T_3 and GC-1 induced thermogenesis, as indicated by increased the body temperature (Figure 3-17A), and elicited weight (Figure 3-17B) and fat loss (Figure 3-17C), although weight and fat loss were significantly greater with GC-1 than T_3. Both compounds elicited similar patterns of gene expression in scWAT (Figure 3-18A), although for all genes profiled, the magnitude of induction was greater for GC-1 than T_3.

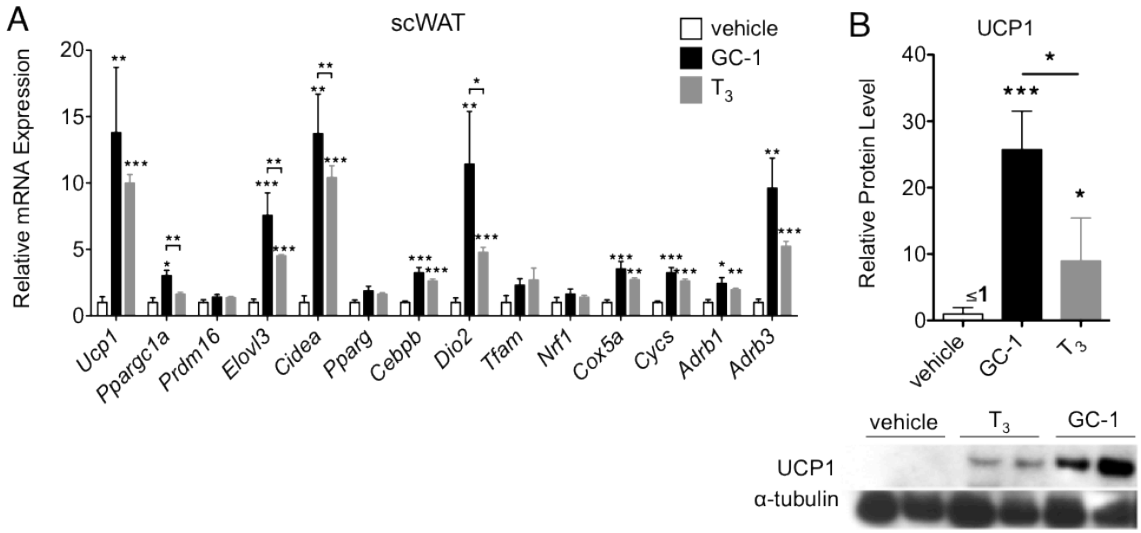

Figure 3-18. Effects of T_3 on the thermogenic genes and UCP1 protein expression in scWAT.
Thermogenic gene (A) and UCP1 protein (B) expression in scWAT of GC-1, T3, or vehicle treated mice (n = 4). Data are mean ± s.e.m. *P < 0.05, **P < 0.01, ***P < 0.001.

Similarly, both ligands strongly increased UCP1 protein levels (Figure 3-18B), although again, the effect was greater with GC-1. Both compounds increased mitochondrial DNA (Figure 3-19A) and citrate synthase activity (Figure 3-19B) in scWAT. In contrast, genes involved in adaptive thermogenesis and UCP1 protein in BAT were almost universally unchanged or repressed by both T_3 and GC-1 (Figure 3-20, A and B). These data demonstrate that TR activation by the endogenous hormone T_3 can elicit a program of adaptive thermogenesis within scWAT.

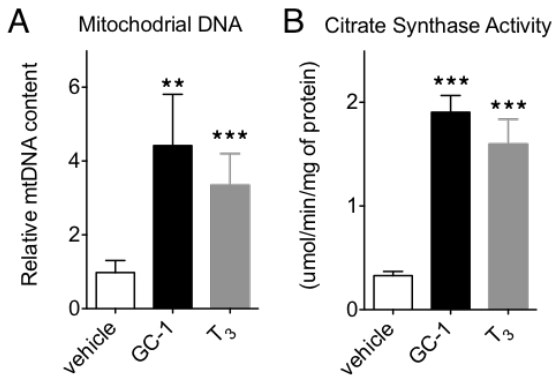

Figure 3-19. T_3 increases mitochondria in scWAT.
Mitochondrial DNA content and citrate synthase activity in scWAT of DIO mice treated with GC-1, T3 or vehicle (*n* = 4). Data are mean ± s.e.m. ***P* < 0.01, ****P* < 0.001.

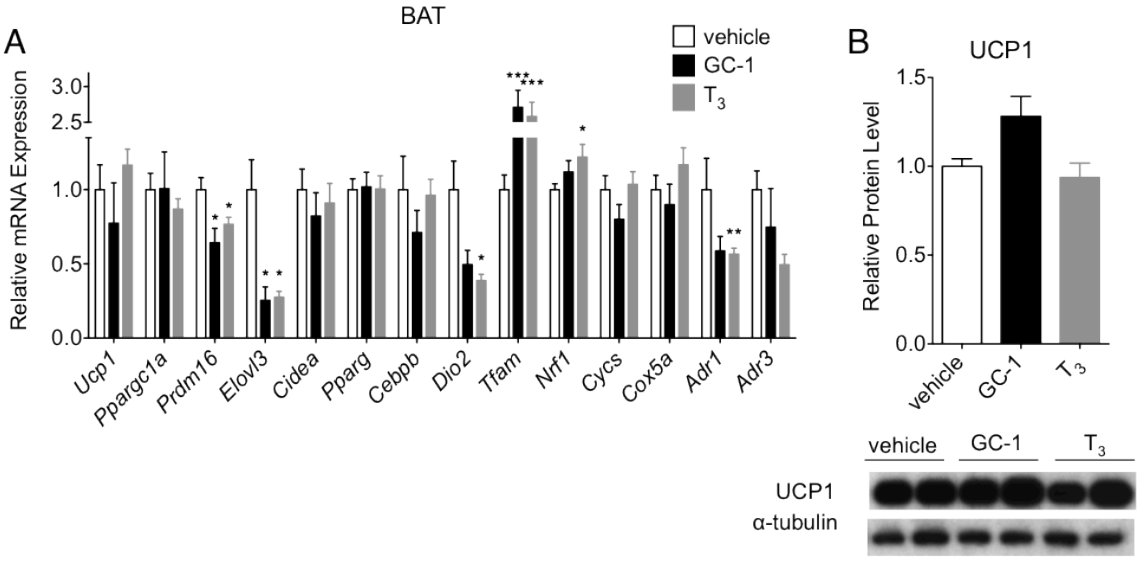

Figure 3-20. Effects of T_3 on the thermogenic genes and UCP1 protein expression in BAT.
Thermogenic gene (A) and UCP1 protein (B) expression in BAT of GC-1, T3, or vehicle treated mice (*n* = 4). Data are mean ± s.e.m. **P* < 0.05, ***P* < 0.01, ****P* < 0.001.

GC-1 Mediated Thermogenesis is Dependent Upon White Adipose Tissue

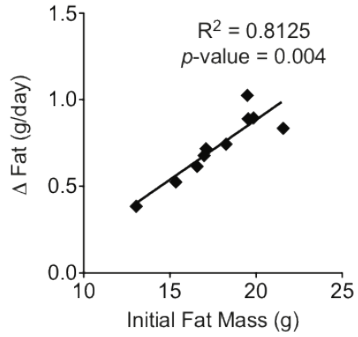

Figure 3-21. Correlation between rate of fat loss and initial fat mass.
Diet-induced obese (DIO) C57Bl/6 mice at 20-24 weeks of age were treated with GC-1. Correlation between adiposity (initial fat mass) and weight loss (Δ Fat) (*n* = 10).

Since our data suggested that the thermogenic effects of TR activation were mediated by a program of adaptive thermogenesis in scWAT, we next asked whether WAT was necessary for the metabolic actions of GC-1. DIO mice of varying levels of adiposity were treated with GC-1 and weight loss was monitored as a surrogate indicator of metabolic increase. The rate of weight loss in these mice was found to correlate strongly with adipose mass (Figure 3-21). Next, we treated lean C57 mice, which had been raised on a chow diet and possessed very little scWAT, with GC-1. Lean mice exhibited no increase in metabolic rates (Figure 3-22, A-C) or elevated body temperature (Figure 3-22D). Contrastingly, obesity induced by high-fat feeding restored the ability of GC-1 to induce thermogenesis in C57 mice, as indicated by increased metabolic rate (Figure 3-22, B and C) and elevated body temperature (Figure 3-22D). Collectively, these

results indicate that triglyceride-rich WAT is necessary for the thermogenic effects of GC-1 and are consistent with the hypothesis that thermogenic induction is mediated by scWAT.

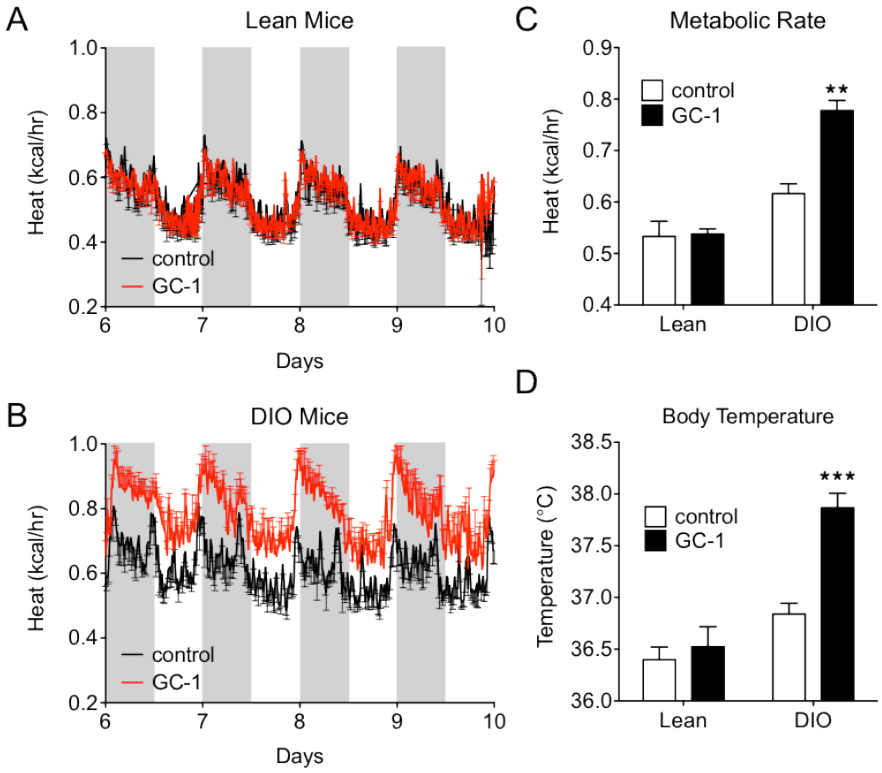

Figure 3-22. GC-1 increases metabolic rate and elevates body temperature in DIO but not lean mice.
Lean and DIO mice at 16 weeks of age were fed, respectively, standard chow or high fat diet with or without GC-1 for 10 days (n = 4 per treatment). Metabolic rate, measured every 15, min in lean mice (A) and DIO mice (B). 72-h average of metabolic rate, day 7-9. (C) and body temperature (D) of lean and DIO C57Bl/6 mice with or without GC-1 treatment. Data are mean ± s.e.m. $^{**}P < 0.01$, $^{***}P < 0.001$.

WAT Browning by TR Agonists is at Least Partially Cell Autonomous

It has been reported that T_3 treatment of human white adipocytes elicits an increase in UCP1 expression and metabolic rate (*45*). In order to test whether the induction of adaptive thermogenesis may be direct action of TR agonists on adipocytes, we tested the ability of T_3 and GC-1 to induce uncoupled respiration and genes involved in adaptive thermogenesis in human and mouse primary cells that had been differentiated into white adipocytes. In mouse adipocytes, GC-1 tended to induce genes involved in adaptive thermogenesis (Figure 3-23A) and uncoupled respiration more than doubled in GC-1-treated adipocytes (Figure 3-23B). Together these results reveal that TR activation can induce uncoupled respiration in white adipocytes in a cell autonomous fashion that does not require central actions.

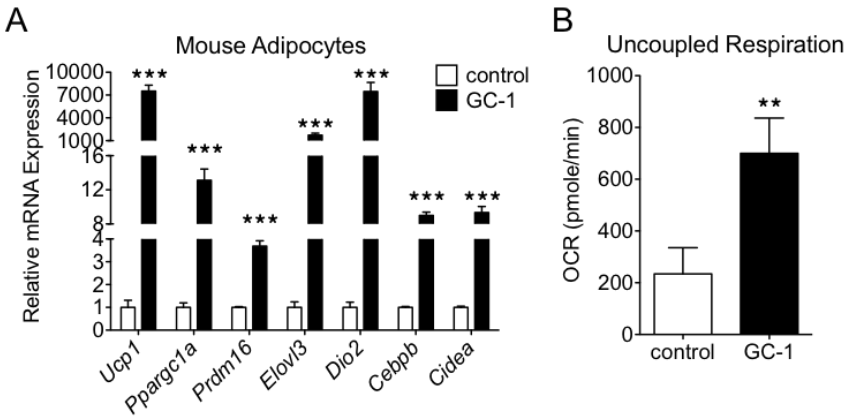

Figure 3-23. GC-1 induces browning of white adipocytes *in vitro*.
The TR agonist GC-1 elicit browning of white adipocytes. Thermogenic gene expression (A) and oxygen consumption rate (B) were measured in mouse stromal-vascular cells isolated from subcutaneous WAT that had been differentiated into adipocytes in the presence or absence of GC-1 (100 μM) (*n* = 4). Data are mean ± s.e.m. **P* < 0.05, ***P* < 0.01, ****P* < 0.001.

DISCUSSION

These data make it clear that TR activation can elicit profound changes in scWAT. Our observations are consistent with recent reports (*135*, *136*) suggesting that various WAT depots possess differing abundances of beige adipocytes, which can be induced to perform UCP1-mediated thermogenesis, and classical white adipocytes, which cannot. Following GC-1 treatment of ob/ob mice, about 40% of subcutaneous white adipocytes exhibit a multilocular BAT-like morphology, which is consistent with the suggestion by Wu et al. (*136*) that thermogenically competent beige cells, or precursors thereof (*137*), comprise about 40% of the adipocytes within scWAT. We found little evidence of GC-1 giving rise to adipocytes within epididymal WAT that possessed brown-like morphology or function, consistent with the idea that adipocytes or adipocyte precursors within this depot have far less potential to conduct UCP1 mediated thermogenesis (*136*, *137*).

While we cannot rule out the possibility that tissues other than scWAT contribute to TR-stimulated thermogenesis, these data strongly suggest that scWAT contributes substantially to the observed thermogenic induction. To our knowledge, the only tissue that is known to be capable of mediating non-shivering thermogenesis of the magnitude observed in the GC-1-treated ob/ob

mice is BAT, leading us to originally suspect that GC-1 must be restoring BAT function to these mice. However, several lines of evidence demonstrate that BAT is not involved in the thermogenesis observed in these mice. Gene expression data, tissue morphology, and functional studies using radiolabeled glucose to measure activity *in vivo* all reveal that BAT activity decreases in GC-1-treated mice. Furthermore, the denervation of interscapular BAT has absolutely no effect on thermogenic induction by GC-1. Collectively, these data indicate that a tissue other than BAT must be responsible for the thermogenic induction observed. It has recently been shown scWAT can at least partially compensate for the loss of BAT (*138*). While essentially all indications of BAT activity were decreased with TR agonist treatment, the same indicators were strongly increased in scWAT, which suggests that TR activation ameliorates the metabolic defects of ob/ob mice, not by restoring BAT activity, but instead by activating a compensatory program of adaptive thermogenesis in scWAT.

Over the past year, numerous studies have demonstrated that a BAT-like program of thermogenesis can be induced within WAT depots, raising the potential of white fat to act as a thermogenic organ (*73*–*76*, *138*). However, the metabolic and physiological changes that have accompanied most demonstrations of WAT browning have been modest, leading some to question the physiological relevance and pharmacological potential of this action (*122*). The magnitude of thermogenesis that accompanied GC-1 treatment and WAT

browning was striking. Initial dose-finding studies with GC-1 elicited a doubling of metabolic rate and chronic hyperthermia (>40°C) in ob/ob mice (data not shown). Could this level of thermogenesis truly be mediated by WAT? Nedergaard and Cannon have put forth a compelling argument that "The only physiologically relevant parameter [in regards to adaptive thermogenesis] is total UCP1 protein level per mouse" (*122*). Following GC-1 treatment, UCP1 transcript and protein levels in scWAT increase by orders of magnitude and approach those found in BAT. Furthermore, since obese mice possess such a large quantity of scWAT, not only do total UCP1 protein levels per mouse rise dramatically (Figure 3-24A), but scWAT becomes the predominant UCP1 containing tissue following GC-1 treatment (Figure 3-24B). A similar calculation, based on transcript levels,

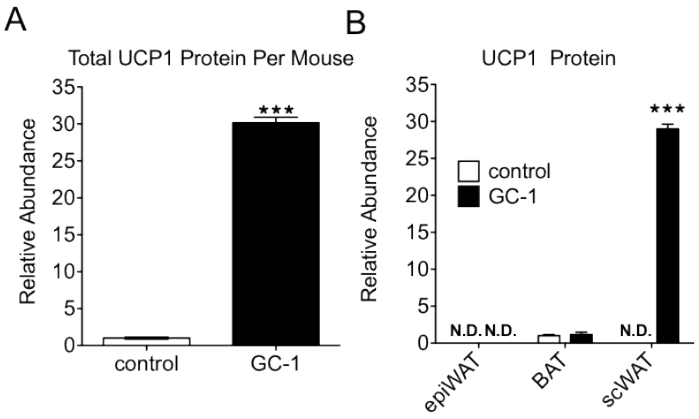

Figure 3-24. UCP1 protein per mouse and per adipose tissue.
(A) Relative total UCP1 protein levels per mouse in ob/ob mice fed 21 days with diets with or without GC-1 (*n* = 4–6). (B) Relative contribution of epiWAT, BAT and scWAT to total mouse UCP1 levels in ob/ob mice treated with GC-1. Data are mean ± s.e.m. ***$P < 0.001$.

estimates that UCP1 levels in GC-1 treated ob/ob mice are about 5-fold higher than those found in BAT of C57 mice (Figure 3-25, A and B), approximating levels found following cold adaptation of these mice. Thus, if UCP1 protein levels

are the best indicator of a tissue's thermogenic capacity, then WAT, and WAT alone, may indeed have capacity to mediate the observed thermogenesis.

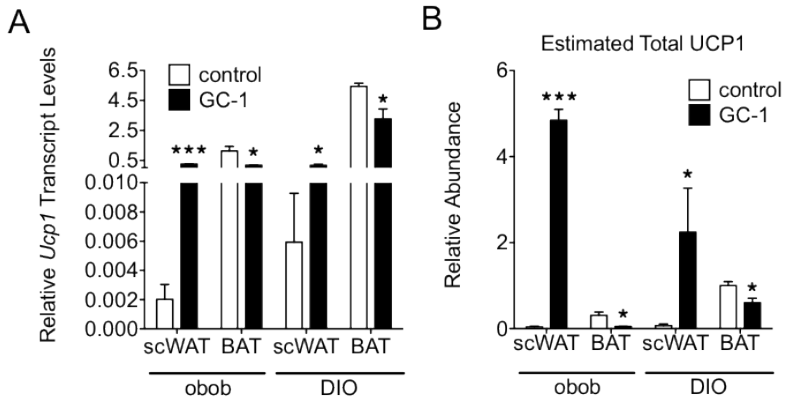

Figure 3-25. Ucp1 transcript and estimated total UCP1 in scWAT and BAT of ob/ob and DIO mice
(A) Relative Ucp1 transcript levels in scWAT and BAT of ob/ob and DIO mice treated with GC-1 (*n* = 4–6). (B) Total UCP1 protein levels per BAT and scWAT adipose depots estimated from relative Ucp1 transcript levels. Data are mean ± s.e.m. **P* < 0.05, ****P* < 0.001.

Given the opposing functions of WAT and BAT, energy storage versus disposal, the conversion of white- to brown-like adipocytes could be expected to effectively reverse the function of WAT. Such changes are indeed observed with GC-1 treatment. Normally, during weight loss, WAT would be expected to be releasing energy via lipolysis. However, GC-1 strongly increases the uptake of energy (glucose) into scWAT in the face of a significant energy deficit. Although not measured in this study, we presume that GC-1 also increases the uptake and metabolism of fatty acids in scWAT, as fatty acids seem to be the preferred substrate for UCP1-mediated thermogenesis (*131*). Consistent with this idea, there is a strong shift towards fatty acid oxidation that coincides with GC-1

treatment and thermogenic induction in WAT. The induction of thermogenesis in WAT coincides with striking improvements in insulin sensitivity and glucose control. Cold activation of BAT thermogenesis has been shown to strongly increase disposal of serum glucose and triglycerides (*139*, *140*). In a similar fashion, our data suggest that WAT thermogenesis can also improve insulin sensitivity and glycemic control by increasing WAT mediated glucose disposal. Notably, the anti-diabetic effects of GC-1 appear to require thermogenic induction, as lower doses that do not induce thermogenesis impair rather than improve glycemic control (*141*). It is tempting to speculate that the striking decreases in serum triglyceride levels that we observed in a prior study when hyperlipidemic mice were treated with GC-1 could be mediated by adaptive thermogenesis driving uptake into WAT (*142*). These results, when analyzed alongside those of Bartelt et al. (*139*), suggest that UCP1-mediated thermogenesis, whether it be conducted by BAT or WAT, has remarkable ability to ameliorate metabolic disease and warrants further exploration.

Mice treated with T_3 or GC-1 become hyperthermic. The basis for the observed hyperthermia is not fully clear. These data, as well as a recent report (*45*), demonstrate that TR activation can induce UCP1 in white adipocytes *in vivo* and *in vitro*. However, increased UCP1 expression is not thought to be sufficient to elicit uncoupled respiration or thermogenesis, as UCP1 is not constitutively active and requires activation by fatty acids that are generated as part of a lipolytic

cascade following β-adrenergic stimulation (*53*). Thus, if we accept that the observed increase in heat production is UCP1 mediated, it follows that either SNS innervation of $UCP1^{+}$ adipocytes must be increased or the requirement for SNS activation is decreased following TR agonism. It has been shown that TRs in the ventromedial hypothalamus are involved in the central regulation of metabolic rate (*143*). Although, in this study, increased metabolic rate was attributed to increased SNS innervation of BAT, it is easy to envision that central TR activation could increase SNS outflow to WAT in a similar fashion. Alternately, a recent report suggests that thermogenesis in beige adipocytes can be induced by an alternative pathway that does not require classical SNS activation via β-adrenergic signaling (*144*). The results here seem to be more consistent with the latter model, that the requirement for SNS stimulation is reduced following TR agonist treatment. That uncoupled respiration increases in cultured adipocytes indicates that, not only is UCP1 expression increased, but that UCP1 is also activated in the absence of any added β-adrenergic agonists. ScWAT levels of norepinephrine do increase in ob/ob mice, but the increase is small and it is difficult to envision that this magnitude of change could mediate the dramatic effects seen in the scWAT of these mice. Also, a similar increase was not observed in DIO mice, despite clear evidence of scWAT browning in these mice.

While TR signaling is clearly implicated in thermogenesis, the browning of WAT has not yet been described as an effect of TR activation *in vivo*. TR-induced thermogenesis is nearly always attributed to BAT, although it is generally acknowledged that tissues other than BAT probably contribute to this action (*126*, *145*). However, our data indicate that functional BAT is not required for TR activation to elicit thermogenesis, since denervation of interscapular BAT, which accounts for the majority of BAT in mice, has no effect on GC-1-mediated thermogenesis in either ob/ob or DIO mice. Conversely, scWAT appears to be required for the thermogenic effects of GC-1 as all thermogenic induction is lost when GC-1 is administered to lean mice that possess little scWAT. Although lean mice do possess white adipocytes, the lack of triglyceride stores within these cells presumably limit their ability to generate intracellular free fatty acids necessary to activate UCP1. Pharmacological doses of T_3 were also able to induce a program of adaptive thermogenesis in scWAT, demonstrating that the browning of WAT is not unique to GC-1 and may, instead, represent a common effect of TR activation in scWAT. Could UCP1 mediated thermogenesis in WAT represent an unappreciated component of 'thyroid thermogenesis'? If WAT mediated thermogenesis were to contribute significantly to systemic thermogenesis elicited by TRs, then the loss of this effect would be expected to result in hypothermia or require a compensatory increase in alternative mechanisms of thermogenesis, such as classical BAT mediated thermogenesis. Indeed, both are common effects of impaired TR signaling and could explain why

the loss of TR signaling due to thyroid ablation, loss of TRs, or loss of DIO2 results in hypothermia and thermogenic defects despite indications of *increased* BAT recruitment, such as increased UCP1 protein (*10*, *16*). This model could also resolve the paradoxical decrease in BAT activity that has been observed by us and others (*146*, *147*), that occurs concomitant with hyperthermia, when rodents are given supraphysiological doses of T_3 or T_4. Thus, we speculate that WAT-mediated thermogenesis may represent a physiologically relevant effect of TR activation that requires functional TR signaling.

In conclusion, TR activation by T_3 and the synthetic agonist GC-1 induces a genetic program of BAT-like thermogenesis and uncoupled respiration in scWAT. TR agonism elicits a functional conversion of WAT into a brown adipose-like tissue that coincides with striking anti-obesity and anti-diabetic actions that we suggest demonstrates the profound pharmacological potential of WAT browning. As GC-1 has been previously shown to evoke rapid weight loss in non-human primates (*32*), we believe that there is strong potential that these results could be translated to man.

Materials and Methods

Animals

Male C57Bl/6 and ob/ob mice were obtained from Harlan Laboratories. Mice were housed in a temperature-controlled environment with 12 h light/dark cycles and fed standard irradiated rodent chow *ad libitum.* At six weeks of age, C57Bl/6 mice were fed a high-fat diet (HFD) containing 0.2% cholesterol (D12079B, Research Diets) for 8 weeks to induce obesity, unless otherwise noted. TR agonists T_3 and GC-1 were administered to 12 week-old ob/ob mice via intraperitoneal injections (0.3 mg/kg/d GC-1, 0.06 mg/kg/d T_3) or admixed in chow (3 mg/kg-diet). Lean and DIO C57B1/6 mice 14-16 weeks of age were administered T_3 or GC-1 via intraperitoneal injections (0.45 mg/kg/d GC-1, 0.3 mg/kg/d T_3) or admixed into chow (3 mg/kg-diet) or HFD (4.8 mg/kg-diet), respectively. Control groups received appropriate vehicle solutions or diets identical to treatment groups. All animal experiments were approved by the Institutional Animal Care and Use Committee of Houston Methodist Research Institute.

BAT Denervation

BAT denervation surgery was performed on ob/ob and C57Bl/6 mice at 3 to 4 weeks of age. Mice were anesthetized with isoflurane and body temperature was maintained with a warming pad. Interscapular BAT lobes were elevated from the

underlying cervical and scapular caudally to separate it from the surrounding muscle and expose sympathetic nerves. The five intercostal nerves of each lobe were isolated and a section of each nerve was removed without damaging the vasculature. The sham procedure was identical except nerves were not transected.

Hyperinsulinemic-Euglycemic Clamp

Hyperinsulinemic-euglycemia clamps were performed at the Mouse Metabolism Core at Baylor College of Medicine. Prior to the clamp, a catheter was inserted into the right internal jugular vein. After recovery, mice were administered GC-1 admixed in diet or control diet for 10-12 days. On the day of the experiment, conscious, overnight-fasted mice received a primed intravenous infusion of ^{3}H-glucose (10 µCi) to measure glucose turnover. The hyperinsulinemic-euglycemic clamp was performed with continuous infusion of insulin (12 mU/kg/min) and variable infusion of glucose to maintain euglycemia. Blood samples were collected every 10 min to measure glucose concentrations. Tissue-specific uptake was performed using ^{14}C-deoxyglucose (10 µCi) 45 min before the end of the clamp experiment.

PET/CT Imaging

^{18}F-deoxyglucose (^{18}F-FDG) (200 µCi) was administered to mice which had received GC-1 via intraperitoneal injection for 14 days. Animals were imaged 1 h

after the injection at the TMHRI preclinical imaging core. microPET/CT imaging was performed using Siemens Inveon dedicated PET and Siemens Inveon multimodality system in docked mode. Anesthetized animals were first subjected to a whole-body CT scan and then to a static ^{18}F PET scan. CT and PET images were aligned and reconstructed with Inveon Research Workplace software (Siemens).

Primary Cell Culture

Mouse subcutaneous preadipocytes were collected from inguinal fat depots of 4-week old C57Bl6 mice as described previously (*148*). Briefly, tissues were digested in PBS containing collagenase I (1.5 mg/ml) and dispase (2.5 mg/ul) at 37°C for 45 min. Undigested tissue and epithelial cells were removed with 100-μm and 40-μm cell strainers, respectively. The stromal vascular cells were cultured in DMEM/F-12 (Invitrogen) containing 10% FBS (Sigma). For adipocyte differentiation, confluent cells were induced in DMEM/F12 containing 10% FBS, isobutulmethylxanthine (IBMX) (0.5 mM), dexamethasone (1 μM), insulin (5 μm/ml), and rosiglitazone (100 nM). After 2 days, cell received fresh media containing 10% FBS and insulin, and the media was changed subsequently every 2 days for 8–9 days. For TR agonist treatment, cells were treated with 100 μM of GC-1 or vehicle during differentiation.

Oxygen Consumption Rate Analysis

Oxygen consumption rates were determined in mouse adipose tissue and subcutaneous adipocytes using a modified protocol (*149*). Inguinal fat depots were extracted from mice and rinsed in XF-DMEM (Seahorse Bioscience) containing 2.5 mM glucose and 1 mM sodium pyruvate. Adipose tissues were cut into small pieces (~10 mg) and rinsed in XF-DMEM media, and immobilized in XF24-well Islet Flux plate (Seahorse Bioscience). Oxygen consumption rate was measured using an Extracellular Flux XF24 analyzer (Seahorse Bioscience) at 37°C. The XF24 Analyzer mixed the media in each well for 2 min before measurements to allow oxygen partial pressure to equilibrate. Basal OCR was measured simultaneously in all wells four times. Tissue replicates from different mice were analyzed in independent experiments and results were normalized to tissue weight. Despite repeated efforts, we were unable to measure uncoupled respiration, presumably due to poor penetrance of oligomycin into the tissue.

For subcutaneous white adipocytes, preadipocytes were plated in a 24-well XF24 cell culture microplates followed by adipocyte differentiation. On the day of the experiment the cells were washed with XF-DMEM and 500 µl of XF-DMEM was added to each well, and the cells were incubated at 37°C without CO_2 for 1 h before the assay. Uncoupled respiration was measured after the addition of oligomycin (2 µg/ml), an ATP synthase inhibitor.

Metabolic Phenotyping

Glucose tolerance tests were performed on mice fasted for 6 h and administered a bolus of glucose (2 g/kg BW) via oral gavage. Blood glucose concentrations were measured at indicated intervals with a standard glucometer (OneTouch). Body composition analysis was performed using noninvasive quantitative NMR (EchoMRI).

Indirect Calorimetry

Metabolic rate, RER, food intake, and ambulatory activity were evaluated by using a Comprehensive Laboratory Animal Monitoring System (Columbus Instruments). Mice were individually housed in metabolic cages with food and water *ad libitum* and allowed to acclimate for 48 h prior to experimentation. Mice were fed chow with or without GC-1 admixed. CO_2 and O_2 levels were measured at 15 min intervals. Metabolic rate, food intake, and ambulatory activity were averaged over 72-h.

Acute Cold Challenge

Mice were individually housed with food and water *ad libitum* and challenged with acute cold at 4°C. Core body temperature was measured prior to cold exposure and at time intervals indicated using a digital thermometer with RET-3 rectal probe for mice.

RNA Extraction and Real-time qPCR

Total RNA was extracted and isolated using QIAzol and RNeasy Mini Kit (Qiagen). First strand cDNA was transcribed from total RNA using SuperScript VILO master mix (Invitrogen). TaqMan real-time PCR reactions were performed on a LightCycler 480 Real-Time PCR system (Roche), and relative mRNA levels were calculated by the comparative Ct method using β-actin as internal control. TaqMan primer/probe sets were supplied by Applied Biosystems. Assay IDs are available upon request.

Mitochondrial DNA Content

RNA-free genomic DNA was isolated from epididymal WAT, subcutaneous WAT and BAT using DNeasy Blood and Tissue Kit (Qiagen). Real-time quantitative qPCR analysis was used to measure the genomic level of mitochondrial NADH dehydrogenase subunit 1 (ND1), which was normalized to nuclear 18S ribosomal DNA.

Histology

Adipose tissues were fixed in 10% buffered formalin, embedded in paraffin, and sectioned at 4 μm. Sections were stained with hematoxylin and eosin.

Adipose Tissue Citrate Synthase Activity

BAT, inguinal WAT, and epididymal WAT were homogenized in CelLytic MT lysis reagent (Sigma) containing a cocktail of protease inhibitors (Roche). Lysates were centrifuged to remove cell debris and lipids. Protein concentration was determined using a NanoDrop spectrophotometer (Thermo Fisher Scientific Inc.). Citrate synthase activity in the protein lysates was measured with a kit (Sigma) following the manufacturer's protocol.

Catecholamines

Norepinephrine content in BAT and inguinal WAT were determined using a commercially available ELISA kit and according to manufacturer's instructions (Rocky Mountain Diagnostics). Tissues were homogenized in buffer containing 1 mM EDTA and 4 mM $Na_2S_2O_5$ to stabilize and prevent degradation of norepinephrine.

Immunoblotting

Adipose tissue was homogenized in tissue extraction reagent (Invitrogen) containing a cocktail of protease inhibitors (Roche). Equivalent amounts of total protein were separated by SDS-PAGE, transferred to polyvinylidene difluoride membranes and probed with antibodies against UCP1 (662045) (Millipore) and α-tubulin (ab7291) (abcam), and with conjugated-HRP anti-rabbit (sc-2004) and

anti-mouse antibodies (sc-2005) (Santa Cruz Biotechnology). Blots were visualized by autoradiography using Amersham ECL Western Blotting Detection Regents (GE Healthcare).

UCP1 Quantification

Relative UCP1 concentrations were calculated by using ImageJ to quantify UCP1 from immunoblots and normalizing to α-tubulin. Total UCP1 protein and *Ucp1* transcripts per tissue were calculated based on the fat mass values obtained by quantitative NMR and multiplied by the relative UCP1 protein or transcript concentration, approximating the fat composition in mice to be 27.8% epididymal WAT, 70% subcutaneous WAT, and 1% (*150*, *151*). Total UCP1 levels per mouse were determined by the sum of UCP1 in epiWAT, scWAT, and BAT.

Statistical Analysis

Data are presented as mean ± s.e.m. A *p*-value of less than 0.05 was considered significant. Student's *t*-test was used for pairwise comparisons. Correlation evaluated by Pearson's correlation coefficient.

CHAPTER 4 CONCLUDING REMARKS AND FUTURE PRESPECTIVES

Thyroid hormones and their receptors were discovered many years ago and their functions have been studied extensively. It has long been known that thyroid hormones regulate many aspects of lipid metabolism and modulation of TRs has been of therapeutic interest to combat obesity and its metabolic complications. TR activation has many effects on lipid metabolism in numerous tissues and work in this thesis was aimed at providing further insights into the effects of TR activation in liver and adipose tissue. We report two novel mechanisms by which TR regulates lipid metabolism: i) thyromimetics lower cholesterol independent of LDLR by increasing bile acid excretion via hepatic Cyp7a1 induction and ii) TR activation by GC-1 induces a functional conversion of white to brown fat. Importantly, both have potential translational implications to treat metabolic diseases such as hyperlipidemia, diabetes, and obesity.

What is the contribution of Cyp7a1 to TR-mediated cholesterol lowering?

The primary mechanism of nearly all cholesterol lowering therapeutics is increasing hepatic cholesterol uptake through the LDLR. This is the mechanism of action of the most commonly prescribed cholesterol drugs, the statins, as well as a new class of cholesterol lowering drugs, PCSK9 inhibitors. Thyroid hormones were also thought to lower cholesterol through stimulating expression of LDLR, however, our data show that TR agonists lower cholesterol via a mechanism that is independent of the LDLR. Thyromimetics lower cholesterol in

LDLR null mice by induction of hepatic Cyp7a1, thus converting cholesterol to bile acids for excretion via reverse cholesterol transport. Our data suggest Cyp7a1 induction may be the primary mechanism of TR-mediated cholesterol reduction. Further studies in Cyp7a1 null mice are warranted to quantitatively address the contribution of Cyp7a1 to the cholesterol reducing actions of TR agonists. This mechanistic distinction is important as Cyp7a overexpression lowers serum cholesterol in rats and rabbits lacking LDLR, which suggests that thyromimetics could be used to treat patients with homozygous familial hypercholesterolemia, who functional LDLR.

What is the physiological relevance of WAT browning?

BAT is generally presumed to be the mechanism by which thyroid hormone induces adaptive thermogenesis; however, the relationship between TR action and BAT activity is complex and contradictory evidence exists. For example, impaired TR signaling results in hypothermia and thermogenic defects despite evidence of increased BAT recruitment and UCP1 protein (*10*, *16*). Similarly, we show that the TR agonist GC-1, which induces thermogenesis, significantly represses BAT activity. Further, we show that TR thermogenesis does not require functional BAT by demonstrating that denervation of interscapular BAT has no effect on GC-1-mediated thermogenesis. Thus we suggest that TR-

mediated thermogenesis can be mediated exclusively by the browning of WAT. This model can potentially resolve some of the confusion regarding the relationship between TR action, BAT, and adaptive thermogenesis, such as the paradoxical decrease in BAT activity that has been previously reported to coincide with thyroid hormone-induced hyperthermia (*146*, *147*)

While it is generally assumed tissues other than BAT probably contribute to thyroid thermogenesis (*126*, *145*), the discovery of alternative mechanisms of thermogenesis have proven elusive. Our data demonstrate that TR activation by GC-1 can functionally convert white to brown fat and induce adaptive thermogenesis in WAT. The contribution of WAT browning to TR thermogenesis should be further studied in knockout mice lacking UCP1 and TRs in WAT and BAT. The browning of white fat is an unrecognized function of TR activation in WAT and may represent a missing component of thyroid thermogenesis.

Does TR-mediated thermogenesis and the browning of WAT require SNS innervation?

The SNS is a major regulator of thermogenesis, as β adrenergic signaling is required to activate a cAMP/PKA/cAMP response element-binding protein signaling cascade, which controls transcription of the thermogenic program. It is well accepted that agonism of β adrenergic receptors that results from cold

exposure activates the thermogenic program in brown and beige fat. Similarly, thyroid hormones have been shown to affect thermogenesis via SNS activation (*143*). However unlike most other examples of beige fat activation, GC-1-induced browning of WAT does not seem to require β-adrenergic stimulation. Two key results strongly suggest that WAT browning by GC-1 is cell autonomous and does not require SNS stimulation: i) the *in vitro* beiging of white preadipocytes in the absence of catecholamine stimulation and ii) the *in vivo* browning of WAT without a large concomitant increase in WAT norepinephrine levels. A recent study in mice that lack all three β-adrenergic receptors (beta-less mice) supports the contention that the browning of white adipocytes is a cell-autonomous action that does not require SNS stimulation (*144*). Whether the SNS is required for TR-mediated WAT browning should be further investigated in beta-less mice. Importantly, since the biggest challenge of adaptive thermogenesis for anti-obesity therapy has been the induction of thermogenic genes is generally insufficient to induce adaptive thermogenesis and β-adrenergic stimulation has always been thought to be additionally required. Thus, a challenge facing the utilization of adaptive thermogenesis as an anti-obesity therapy has been the question of how to simultaneous induce the thermogenic program and also activate it. However, our data indicates that the TR agonist GC-1 both induces and activates adaptive thermogenesis, which suggests that TR agonist-mediated WAT browning could represent an effective strategy to combat metabolic disease.

CHAPTER 5 REFERENCES

1. J. H. Oppenheimer *et al.*, Advances in our understanding of thyroid hormone action at the cellular level, *Endocr. Rev.* **8**, 288–308 (1987).

2. M. A. Shupnik, E. C. Ridgway, W. W. Chin, Molecular biology of thyrotropin, *Endocr. Rev.* **10**, 459–475 (1989).

3. E. C. H. Friesema, J. Jansen, C. Milici, T. J. Visser, Thyroid hormone transporters, *Vitam. Horm.* **70**, 137–167 (2005).

4. A. C. Bianco, D. Salvatore, B. Gereben, M. J. Berry, P. R. Larsen, Biochemistry, cellular and molecular biology, and physiological roles of the iodothyronine selenodeiodinases, *Endocr. Rev.* **23**, 38–89 (2002).

5. M. Beato, P. Herrlich, G. Schütz, Steroid hormone receptors: many actors in search of a plot, *Cell* **83**, 851–857 (1995).

6. M. A. Lazar, Thyroid hormone receptors: multiple forms, multiple possibilities, *Endocr. Rev.* **14**, 184–193 (1993).

7. P. M. Yen, Physiological and molecular basis of thyroid hormone action, *Physiol. Rev.* **81**, 1097–1142 (2001).

8. D. Forrest, L. C. Erway, L. Ng, R. Altschuler, T. Curran, Thyroid hormone receptor beta is essential for development of auditory function, *Nat. Genet.* **13**, 354–357 (1996).

9. S. Göthe *et al.*, Mice devoid of all known thyroid hormone receptors are viable but exhibit disorders of the pituitary–thyroid axis, growth, and bone maturation, *Genes Dev.* **13**, 1329–1341 (1999).

10. L. Wikström *et al.*, Abnormal heart rate and body temperature in mice lacking thyroid hormone receptor alpha 1, *EMBO J.* **17**, 455–461 (1998).

11. M. Sjögren *et al.*, Hypermetabolism in mice caused by the central action of an unliganded thyroid hormone receptor alpha1, *EMBO J.* **26**, 4535–4545 (2007).

12. M. Kaneshige *et al.*, A targeted dominant negative mutation of the thyroid hormone alpha 1 receptor causes increased mortality, infertility, and dwarfism in mice, *Proc. Natl. Acad. Sci. U. S. A.* **98**, 15095–15100 (2001).

13. H. Ying, O. Araki, F. Furuya, Y. Kato, S.-Y. Cheng, Impaired adipogenesis caused by a mutated thyroid hormone alpha1 receptor, *Mol. Cell. Biol.* **27**, 2359–2371 (2007).

14. L. Quignodon, S. Vincent, H. Winter, J. Samarut, F. Flamant, A point mutation in the activation function 2 domain of thyroid hormone receptor alpha1 expressed after CRE-mediated recombination partially recapitulates hypothyroidism, *Mol. Endocrinol. Baltim. Md* **21**, 2350–2360 (2007).

15. T. Endo, T. Kobayashi, Thyroid-stimulating hormone receptor in brown adipose tissue is involved in the regulation of thermogenesis, *Am. J. Physiol. Endocrinol. Metab.* **295**, E514–518 (2008).

16. V. Golozoubova, Depressed thermogenesis but competent brown adipose tissue recruitment in mice devoid of all hormone-binding thyroid hormone rxeceptors, *Mol. Endocrinol.* **18**, 384–401 (2003).

17. Y.-Y. Liu, J. J. Schultz, G. A. Brent, A thyroid hormone receptor alpha gene mutation (P398H) is associated with visceral adiposity and impaired catecholamine-stimulated lipolysis in mice, *J. Biol. Chem.* **278**, 38913–38920 (2003).

18. J. S. Melish, in *Clinical Methods: The History, Physical, and Laboratory Examinations*, H. K. Walker, W. D. Hall, J. W. Hurst, Eds. (Butterworths, Boston, 1990).

19. A. M. Dumitrescu, X.-H. Liao, T. B. Best, K. Brockmann, S. Refetoff, A novel syndrome combining thyroid and neurological abnormalities is associated with mutations in a monocarboxylate transporter gene, *Am. J. Hum. Genet.* **74**, 168–175 (2004).

20. E. C. H. Friesema *et al.*, Association between mutations in a thyroid hormone transporter and severe X-linked psychomotor retardation, *Lancet* **364**, 1435–1437 (2004).

21. A. M. Dumitrescu *et al.*, Mutations in SECISBP2 result in abnormal thyroid hormone metabolism, *Nat. Genet.* **37**, 1247–1252 (2005).

22. C. Baigent *et al.*, Efficacy and safety of cholesterol-lowering treatment: prospective meta-analysis of data from 90,056 participants in 14 randomised trials of statins, *Lancet* **366**, 1267–1278 (2005).

23. M. S. Brown, J. L. Goldstein, The SREBP pathway: regulation of cholesterol metabolism by proteolysis of a membrane-bound transcription factor, *Cell* **89**, 331–340 (1997).

24. R. Mason, H. Hunt, L. Hurxthal, Blood cholesterol values in hyperthyroidism and hypothyroidism their significance, *N. Engl. J. Med.* **203**, 1273–8 (1930).

25. G. R. Thompson *et al.*, Defects of receptor-mediated low density lipoprotein catabolism in homozygous familial hypercholesterolemia and hypothyroidism in vivo, *Proc. Natl. Acad. Sci. U. S. A.* **78**, 2591–2595 (1981).

26. G. C. Ness, L. C. Pendleton, Y. C. Li, J. Y. Chiang, Effect of thyroid hormone on hepatic cholesterol 7 alpha hydroxylase, LDL receptor, HMG-CoA reductase, farnesyl pyrophosphate synthetase and apolipoprotein A-I mRNA levels in hypophysectomized rats, *Biochem. Biophys. Res. Commun.* **172**, 1150–1156 (1990).

27. H. Gullberg *et al.*, Requirement for thyroid hormone receptor beta in T3 regulation of cholesterol metabolism in mice, *Mol. Endocrinol. Baltim. Md* **16**, 1767–1777 (2002).

28. L. E. Braverman, D. S. Cooper, *Werner and Ingbar's. The Thyroid: A Fundamental and Clinical Text.* (Lippincott Williams & Wilkins, Philadelphia, 2012).

29. J. Stamler, The coronary drug project--findings with regard to estrogen, dextrothyroxine, clofibrate and niacin, *Adv. Exp. Med. Biol.* **82**, 52–75 (1977).

30. R. Day *et al.*, Time course of hepatic 3-hydroxy-3-methylglutaryl coenzyme A reductase activity and messenger ribonucleic acid, biliary lipid secretion, and hepatic cholesterol content in methimazole-treated hypothyroid and hypophysectomized rats after triiodothyronine administration: possible linkage of cholesterol synthesis to biliary secretion, *Endocrinology* **125**, 459–468 (1989).

31. E. H. Strisower, B. Strisower, The separate hypolipoproteinemic effects of dextrothyroxine and ethyl chlorophenoxyisobutyrate, *J. Clin. Endocrinol. Metab.* **24**, 139–144 (1964).

32. G. J. Grover, Effects of the thyroid hormone receptor agonist GC-1 on metabolic rate and cholesterol in rats and primates: selective actions relative to 3,5,3'-triiodo-L-thyronine, *Endocrinology* **145**, 1656–1661 (2003).

33. E. Morkin *et al.*, Pilot studies on the use of 3,5-diiodothyropropionic acid, a thyroid hormone analog, in the treatment of congestive heart failure, *Cardiology* **97**, 218–225 (2002).

34. G. C. Ness, Z. Zhao, Thyroid hormone rapidly induces hepatic LDL receptor mRNA levels in hypophysectomized rats, *Arch. Biochem. Biophys.* **315**, 199–202 (1994).

35. H. Shimano *et al.*, Overproduction of cholesterol and fatty acids causes massive liver enlargement in transgenic mice expressing truncated SREBP-1a, *J. Clin. Invest.* **98**, 1575–1584 (1996).

36. J. D. Baxter, P. Webb, G. Grover, T. S. Scanlan, Selective activation of thyroid hormone signaling pathways by GC-1: a new approach to controlling cholesterol and body weight, *Trends Endocrinol. Metab. TEM* **15**, 154–157 (2004).

37. M. S. Brown, J. L. Goldstein, A receptor-mediated pathway for cholesterol homeostasis, *Science* **232**, 34–47 (1986).

38. M. D. Erion *et al.*, Targeting thyroid hormone receptor-beta agonists to the liver reduces cholesterol and triglycerides and improves the therapeutic index, *Proc. Natl. Acad. Sci. U. S. A.* **104**, 15490–15495 (2007).

39. G. C. Ness *et al.*, Effects of L-triiodothyronine and the thyromimetic L-94901 on serum lipoprotein levels and hepatic low-density lipoprotein receptor, 3-hydroxy-3-methylglutaryl coenzyme A reductase, and apo A-I gene expression, *Biochem. Pharmacol.* **56**, 121–129 (1998).

40. L. Johansson *et al.*, Selective thyroid receptor modulation by GC-1 reduces serum lipids and stimulates steps of reverse cholesterol transport in euthyroid mice, *Proc. Natl. Acad. Sci. U. S. A.* **102**, 10297 –10302 (2005).

41. I. Tancevski *et al.*, The liver-selective thyromimetic T-0681 influences reverse cholesterol transport and atherosclerosis development in mice, *PloS One* **5**, e8722 (2010).

42. J. E. Silva, Thyroid hormone control of thermogenesis and energy balance, *Thyroid Off. J. Am. Thyroid Assoc.* **5**, 481–492 (1995).

43. L. A. de Jesus *et al.*, The type 2 iodothyronine deiodinase is essential for adaptive thermogenesis in brown adipose tissue, *J. Clin. Invest.* **108**, 1379–1385 (2001).

44. A. M. Cassard-Doulcier *et al.*, In vitro interactions between nuclear proteins and uncoupling protein gene promoter reveal several putative

transactivating factors including Ets1, retinoid X receptor, thyroid hormone receptor, and a CACCC box-binding protein, *J. Biol. Chem.* **269**, 24335–24342 (1994).

45. J.-Y. Lee *et al.*, Triiodothyronine induces UCP-1 expression and mitochondrial biogenesis in human adipocytes, *Am. J. Physiol. - Cell Physiol.* **302**, C463–C472 (2012).

46. L. A. Videla, V. Fernández, G. Tapia, P. Varela, Thyroid hormone calorigenesis and mitochondrial redox signaling: upregulation of gene expression, *Front. Biosci. J. Virtual Libr.* **12**, 1220–1228 (2007).

47. T. J. Connelly, R. el-Hayek, M. Sukhareva, R. Coronado, L-thyroxine activates the intracellular Ca2+ release channel of skeletal muscle sarcoplasmic reticulum, *Biochem. Mol. Biol. Int.* **32**, 441–448 (1994).

48. W. S. Simonides, M. H. Thelen, C. G. van der Linden, A. Muller, C. van Hardeveld, Mechanism of thyroid-hormone regulated expression of the SERCA genes in skeletal muscle: implications for thermogenesis, *Biosci. Rep.* **21**, 139–154 (2001).

49. G. I. Shulman, P. W. Ladenson, M. H. Wolfe, E. C. Ridgway, R. R. Wolfe, Substrate cycling between gluconeogenesis and glycolysis in euthyroid, hypothyroid, and hyperthyroid man, *J. Clin. Invest.* **76**, 757–764 (1985).

50. K. F. Petersen, G. W. Cline, J. B. Blair, G. I. Shulman, Substrate cycling between pyruvate and oxaloacetate in awake normal and 3,3'-5-triiodo-L-thyronine-treated rats, *Am. J. Physiol.* **267**, E273–277 (1994).

51. K. F. Petersen, J. B. Blair, G. I. Shulman, Triiodothyronine treatment increases substrate cycling between pyruvate carboxylase and malic enzyme in perfused rat liver, *Metabolism.* **44**, 1380–1383 (1995).

52. S. Klein *et al.*, Waist circumference and cardiometabolic risk: a consensus statement from shaping America's health: Association for Weight Management and Obesity Prevention; NAASO, the Obesity Society; the American Society for Nutrition; and the American Diabetes Association, *Diabetes Care* **30**, 1647–1652 (2007).

53. B. Cannon, J. Nedergaard, Brown adipose tissue: function and physiological significance, *Physiol. Rev.* **84**, 277–359 (2004).

54. S. R. Farmer, Molecular determinants of brown adipocyte formation and function, *Genes Dev.* **22**, 1269–1275 (2008).

55. P. Seale, S. Kajimura, B. M. Spiegelman, Transcriptional control of brown adipocyte development and physiological function--of mice and men, *Genes Dev.* **23**, 788–797 (2009).

56. Y. Wang, E. B. Rimm, M. J. Stampfer, W. C. Willett, F. B. Hu, Comparison of abdominal adiposity and overall obesity in predicting risk of type 2 diabetes among men, *Am. J. Clin. Nutr.* **81**, 555–563 (2005).

57. C. S. Fox *et al.*, Abdominal visceral and subcutaneous adipose tissue compartments: association with metabolic risk factors in the Framingham Heart Study, *Circulation* **116**, 39–48 (2007).

58. J. P. Després *et al.*, The insulin resistance-dyslipidemic syndrome: contribution of visceral obesity and therapeutic implications, *Int. J. Obes. Relat. Metab. Disord. J. Int. Assoc. Study Obes.* **19 Suppl 1**, S76–86 (1995).

59. R. Ross, L. Fortier, R. Hudson, Separate associations between visceral and subcutaneous adipose tissue distribution, insulin and glucose levels in obese women, *Diabetes Care* **19**, 1404–1411 (1996).

60. K. M. Rexrode *et al.*, Abdominal adiposity and coronary heart disease in women, *JAMA J. Am. Med. Assoc.* **280**, 1843–1848 (1998).

61. S. A. Porter *et al.*, Abdominal subcutaneous adipose tissue: a protective fat depot?, *Diabetes Care* **32**, 1068–1075 (2009).

62. M. B. Snijder *et al.*, Low subcutaneous thigh fat is a risk factor for unfavourable glucose and lipid levels, independently of high abdominal fat. The Health ABC Study, *Diabetologia* **48**, 301–308 (2005).

63. Y. Miyazaki *et al.*, Effect of pioglitazone on abdominal fat distribution and insulin sensitivity in type 2 diabetic patients, *J. Clin. Endocrinol. Metab.* **87**, 2784–2791 (2002).

64. S. Klein *et al.*, Absence of an effect of liposuction on insulin action and risk factors for coronary heart disease, *N. Engl. J. Med.* **350**, 2549–2557 (2004).

65. L. B. Tankó, Y. Z. Bagger, P. Alexandersen, P. J. Larsen, C. Christiansen, Peripheral adiposity exhibits an independent dominant antiatherogenic effect in elderly women, *Circulation* **107**, 1626–1631 (2003).

66. B. B. Lowell *et al.*, Development of obesity in transgenic mice after genetic ablation of brown adipose tissue, *Nature* **366**, 740–742 (1993).

67. E. S. Bachman *et al.*, betaAR signaling required for diet-induced thermogenesis and obesity resistance, *Science* **297**, 843–845 (2002).

68. M. C. Zingaretti *et al.*, The presence of UCP1 demonstrates that metabolically active adipose tissue in the neck of adult humans truly represents brown adipose tissue, *FASEB J.* **23**, 3113–3120 (2009).

69. W. D. van Marken Lichtenbelt *et al.*, Cold-activated brown adipose tissue in healthy men, *N. Engl. J. Med.* **360**, 1500–1508 (2009).

70. A. M. Cypess *et al.*, Identification and importance of brown adipose tissue in adult humans, *N. Engl. J. Med.* **360**, 1509–1517 (2009).

71. K. A. Virtanen *et al.*, Functional brown adipose tissue in healthy adults, *N. Engl. J. Med.* **360**, 1518–1525 (2009).

72. J. Nedergaard, T. Bengtsson, B. Cannon, Unexpected evidence for active brown adipose tissue in adult humans, *Am. J. Physiol. - Endocrinol. Metab.* **293**, E444–E452 (2007).

73. P. Boström *et al.*, A PGC1-α-dependent myokine that drives brown-fat-like development of white fat and thermogenesis, *Nature* **481**, 463–468 (2012).

74. M. Bordicchia *et al.*, Cardiac natriuretic peptides act via p38 MAPK to induce the brown fat thermogenic program in mouse and human adipocytes, *J. Clin. Invest.* **122**, 1022–1036 (2012).

75. F. W. Kiefer *et al.*, Retinaldehyde dehydrogenase 1 regulates a thermogenic program in white adipose tissue, *Nat. Med.* **18**, 918–925 (2012).

76. F. M. Fisher *et al.*, FGF21 regulates PGC-1 and browning of white adipose tissues in adaptive thermogenesis, *Genes Dev.* **26**, 271–281 (2012).

77. B. Cousin *et al.*, Occurrence of brown adipocytes in rat white adipose tissue: molecular and morphological characterization, *J. Cell Sci.* **103**, 931–942 (1992).

78. M. Ghorbani, J. Himms-Hagen, Appearance of brown adipocytes in white adipose tissue during CL 316,243-induced reversal of obesity and diabetes in Zucker fa/fa rats, *Int. J. Obes. Relat. Metab. Disord. J. Int. Assoc. Study Obes.* **21**, 465–475 (1997).

79. C. Guerra, R. A. Koza, H. Yamashita, K. Walsh, L. P. Kozak, Emergence of brown adipocytes in white fat in mice is under genetic control. Effects on body weight and adiposity., *J. Clin. Invest.* **102**, 412–420 (1998).

80. J. Himms-Hagen *et al.*, Multilocular fat cells in WAT of CL-316243-treated rats derive directly from white adipocytes, *Am. J. Physiol. - Cell Physiol.* **279**, C670–C681 (2000).

81. P. Huttunen, J. Hirvonen, V. Kinnula, The occurrence of brown adipose tissue in outdoor workers, *Eur. J. Appl. Physiol.* **46**, 339–345 (1981).

82. B. Xue, A. Coulter, J. S. Rim, R. A. Koza, L. P. Kozak, Transcriptional synergy and the regulation of Ucp1 during brown adipocyte induction in white fat depots, *Mol. Cell. Biol.* **25**, 8311–8322 (2005).

83. G. Barbatelli *et al.*, The emergence of cold-induced brown adipocytes in mouse white fat depots is determined predominantly by white to brown adipocyte transdifferentiation, *Am. J. Physiol. Endocrinol. Metab.* **298**, E1244–1253 (2010).

84. S. Collins, K. W. Daniel, A. E. Petro, R. S. Surwit, Strain-specific response to beta 3-adrenergic receptor agonist treatment of diet-induced obesity in mice, *Endocrinology* **138**, 405–413 (1997).

85. P. Seale *et al.*, PRDM16 controls a brown fat/skeletal muscle switch, *Nature* **454**, 961–967 (2008).

86. J. Goldstein, H. Hobbs, M. Brown, in *The Metabolic and Molecular Bases of Inherited Disease*, (McGraw-Hill Book Co, New York, 2001).

87. J. D. Baxter, P. Webb, Thyroid hormone mimetics: potential applications in atherosclerosis, obesity and type 2 diabetes, *Nat. Rev. Drug Discov.* **8**, 308–320 (2009).

88. S. U. Trost *et al.*, The thyroid hormone receptor-beta-selective agonist GC-1 differentially affects plasma lipids and cardiac activity, *Endocrinology* **141**, 3057–3064 (2000).

89. A. Honda *et al.*, Significance of plasma 7alpha-hydroxy-4-cholesten-3-one and 27-hydroxycholesterol concentrations as markers for hepatic bile acid synthesis in cholesterol-fed rabbits, *Metabolism.* **53**, 42–48 (2004).

90. T. Kanda *et al.*, Regulation of expression of human intestinal bile acid-binding protein in Caco-2 cells., *Biochem. J.* **330**, 261 (1998).

91. B. G. Bhat *et al.*, Inhibition of ileal bile acid transport and reduced atherosclerosis in apoE-/- mice by SC-435, *J. Lipid Res.* **44**, 1614–1621 (2003).

92. L. Yu *et al.*, Overexpression of ABCG5 and ABCG8 promotes biliary cholesterol secretion and reduces fractional absorption of dietary cholesterol, *J. Clin. Invest.* **110**, 671–680 (2002).

93. A. Rao *et al.*, The organic solute transporter alpha-beta, Ostalpha-Ostbeta, is essential for intestinal bile acid transport and homeostasis, *Proc. Natl. Acad. Sci. U. S. A.* **105**, 3891–3896 (2008).

94. L. Yu *et al.*, Disruption of Abcg5 and Abcg8 in mice reveals their crucial role in biliary cholesterol secretion, *Proc. Natl. Acad. Sci. U. S. A.* **99**, 16237–16242 (2002).

95. S. Zadelaar *et al.*, Mouse models for atherosclerosis and pharmaceutical modifiers, *Arterioscler. Thromb. Vasc. Biol.* **27**, 1706–1721 (2007).

96. N. O. Davidson, R. C. Carlos, M. J. Drewek, T. G. Parmer, Apolipoprotein gene expression in the rat is regulated in a tissue-specific manner by thyroid hormone., *J. Lipid Res.* **29**, 1511–1522 (1988).

97. A. Theriault, G. Ogbonna, K. Adeli, Thyroid hormone modulates apolipoprotein B gene expression in HepG2 cells, *Biochem. Biophys. Res. Commun.* **186**, 617–623 (1992).

98. J. H. Miyake *et al.*, Increased production of apolipoprotein B-containing lipoproteins in the absence of hyperlipidemia in transgenic mice expressing cholesterol 7alpha-hydroxylase, *J. Biol. Chem.* **276**, 23304–23311 (2001).

99. G. Xu *et al.*, Increasing hepatic cholesterol 7alpha-hydroxylase reduces plasma cholesterol concentrations in normocholesterolemic and hypercholesterolemic rabbits, *Hepatol. Baltim. Md* **24**, 882–887 (1996).

100. E. P. Ratliff, A. Gutierrez, R. A. Davis, Transgenic expression of CYP7A1 in LDL receptor-deficient mice blocks diet-induced hypercholesterolemia, *J. Lipid Res.* **47**, 1513–1520 (2006).

101. D. K. Spady, J. A. Cuthbert, M. N. Willard, R. S. Meidell, Overexpression of cholesterol 7alpha-hydroxylase (CYP7A) in mice lacking the low density lipoprotein (LDL) receptor gene. LDL transport and plasma LDL concentrations are reduced, *J. Biol. Chem.* **273**, 126–132 (1998).

102. D. K. Spady, J. A. Cuthbert, M. N. Willard, R. S. Meidell, Adenovirus-mediated transfer of a gene encoding cholesterol 7 alpha-hydroxylase into hamsters increases hepatic enzyme activity and reduces plasma total and low density lipoprotein cholesterol, *J. Clin. Invest.* **96**, 700–709 (1995).

103. C. E. Sample, L. C. Pendleton, G. C. Ness, Regulation of 3-hydroxy-3-methylglutaryl coenzyme A reductase mRNA levels by L-triiodothyronine, *Biochemistry (Mosc.)* **26**, 727–731 (1987).

104. S. M. Post, M. Groenendijk, K. Solaas, P. C. N. Rensen, H. M. G. Princen, Cholesterol 7alpha-hydroxylase deficiency in mice on an APOE*3-Leiden background impairs very-low-density lipoprotein production, *Arterioscler. Thromb. Vasc. Biol.* **24**, 768–774 (2004).

105. D.-J. Shin, M. Plateroti, J. Samarut, T. F. Osborne, Two uniquely arranged thyroid hormone response elements in the far upstream 5' flanking region confer direct thyroid hormone regulation to the murine cholesterol 7alpha hydroxylase gene, *Nucleic Acids Res.* **34**, 3853–3861 (2006).

106. G. C. Ness, D. Lopez, Transcriptional regulation of rat hepatic low-density lipoprotein receptor and cholesterol 7 alpha hydroxylase by thyroid hormone, *Arch. Biochem. Biophys.* **323**, 404–408 (1995).

107. C. R. Pullinger *et al.*, Human cholesterol 7α-hydroxylase (CYP7A1) deficiency has a hypercholesterolemic phenotype, *J. Clin. Invest.* **110**, 109–117 (2002).

108. V. A. B. Drover, L. B. Agellon, Regulation of the human cholesterol 7alpha-hydroxylase gene (CYP7A1) by thyroid hormone in transgenic mice, *Endocrinology* **145**, 574–581 (2004).

109. A. Berkenstam *et al.*, The thyroid hormone mimetic compound KB2115 lowers plasma LDL cholesterol and stimulates bile acid synthesis without cardiac effects in humans, *Proc. Natl. Acad. Sci.* **105**, 663 –667 (2008).

110. P. W. Ladenson *et al.*, Use of the thyroid hormone analogue eprotirome in statin-treated dyslipidemia, *N. Engl. J. Med.* **362**, 906–916 (2010).

111. A. Honda *et al.*, Highly sensitive quantification of 7alpha-hydroxy-4-cholesten-3-one in human serum by LC-ESI-MS/MS, *J. Lipid Res.* **48**, 458–464 (2007).

112. E. Voyiaziakis, C. Ko, S. M. O'Rourke, L. S. Huang, Genetic control of hepatic apoB-100 secretion in human apoB transgenic mouse strains, *J. Lipid Res.* **40**, 2004–2012 (1999).

113. World Health Organization, Obesity and Overweight: Fact Sheet (2013) (available at http://www.who.int/mediacentre/factsheets/fs311/en/).

114. P. Puigserver *et al.*, A cold-inducible coactivator of nuclear receptors linked to adaptive thermogenesis, *Cell* **92**, 829–839 (1998).

115. P. Trayhurn, J. H. Beattie, Physiological role of adipose tissue: white adipose tissue as an endocrine and secretory organ, *Proc. Nutr. Soc.* **60**, 329–339 (2001).

116. V. Golozoubova, B. Cannon, J. Nedergaard, UCP1 is essential for adaptive adrenergic nonshivering thermogenesis, *Am. J. Physiol. Endocrinol. Metab.* **291**, E350–357 (2006).

117. D. G. Nicholls, R. M. Locke, Thermogenic mechanisms in brown fat., *Physiol. Rev.* **64**, 1–64 (1984).

118. J. Himms-Hagen, Brown adipose tissue thermogenesis and obesity, *Prog. Lipid Res.* **28**, 67–115 (1989).

119. C. Tiraby, D. Langin, Conversion from white to brown adipocytes: a strategy for the control of fat mass?, *Trends Endocrinol. Metab.* **14**, 439–441 (2003).

120. D. Lonc̆ar, B. A. Afzelius, B. Cannon, Epididymal white adipose tissue after cold stress in rats II. Mitochondrial changes, *J. Ultrastruct. Mol. Struct. Res.* **101**, 199–209 (1988).

121. J. R. S. Arch, The discovery of drugs for obesity, the metabolic effects of leptin and variable receptor pharmacology: perspectives from beta3-adrenoceptor agonists, *Naunyn. Schmiedebergs Arch. Pharmacol.* **378**, 225–240 (2008).

122. J. Nedergaard, B. Cannon, UCP1 mRNA does not produce heat, *Biochim. Biophys. Acta BBA - Mol. Cell Biol. Lipids* (2013), doi:10.1016/j.bbalip.2013.01.009.

123. D. Guernsey, I. Edelman, in *Molecular Basis of Thyroid Hormone Action*, (Academic Press, Inc, 1983), pp. 293–324.

124. H. Ohno, K. Shinoda, B. M. Spiegelman, S. Kajimura, PPARγ agonists induce a white-to-brown fat conversion through stabilization of PRDM16 protein, *Cell Metab.* **15**, 395–404 (2012).

125. M. A. Christoffolete *et al.*, Mice with targeted disruption of the Dio2 gene have cold-induced overexpression of the uncoupling protein 1 gene but fail to increase brown adipose tissue lipogenesis and adaptive thermogenesis, *Diabetes* **53**, 577–584 (2004).

126. B. B. Lowell, B. M. Spiegelman, Towards a molecular understanding of adaptive thermogenesis, *Nature* **404**, 652–660 (2000).

127. L. de Meis, A. P. Arruda, D. P. Carvalho, Role of sarco/endoplasmic reticulum Ca(2+)-ATPase in thermogenesis, *Biosci. Rep.* **25**, 181–190 (2005).

128. S. Cinti, M. C. Zingaretti, R. Cancello, E. Ceresi, P. Ferrara, in *Adipose Tissue Protocols*, (Humana Press, New Jersey, 2001), vol. 155, pp. 21–51.

129. P. Seale *et al.*, Prdm16 determines the thermogenic program of subcutaneous white adipose tissue in mice, *J. Clin. Invest.* **121**, 96–105 (2011).

130. B. Cannon, J. Nedergaard, Thermogenesis challenges the adipostat hypothesis for body-weight control, *Proc. Nutr. Soc.* **68**, 401 (2009).

131. K. D. Nguyen *et al.*, Alternatively activated macrophages produce catecholamines to sustain adaptive thermogenesis, *Nature* **480**, 104–108 (2011).

132. E. Ioffe, B. Moon, E. Connolly, J. M. Friedman, Abnormal regulation of the leptin gene in the pathogenesis of obesity, *Proc. Natl. Acad. Sci.* **95**, 11852–11857 (1998).

133. B. Cannon, J. Nedergaard, Nonshivering thermogenesis and its adequate measurement in metabolic studies, *J. Exp. Biol.* **214**, 242–253 (2011).

134. M. O. Ribeiro *et al.*, Thyroid hormone--sympathetic interaction and adaptive thermogenesis are thyroid hormone receptor isoform--specific, *J. Clin. Invest.* **108**, 97–105 (2001).

135. A. M. Cypess *et al.*, Anatomical localization, gene expression profiling and functional characterization of adult human neck brown fat, *Nat. Med.* **19**, 635–639 (2013).

136. J. Wu *et al.*, Beige adipocytes are a distinct type of thermogenic fat cell in mouse and human, *Cell* **150**, 366–376 (2012).

137. Q. A. Wang, C. Tao, R. K. Gupta, P. E. Scherer, Tracking adipogenesis during white adipose tissue development, expansion and regeneration, *Nat. Med.* **19**, 1338–1344 (2013).

138. T. J. Schulz *et al.*, Brown-fat paucity due to impaired BMP signalling induces compensatory browning of white fat, *Nature* **495**, 379–383 (2013).

139. A. Bartelt *et al.*, Brown adipose tissue activity controls triglyceride clearance, *Nat. Med.* **17**, 200–205 (2011).

140. J. Nedergaard, T. Bengtsson, B. Cannon, New powers of brown fat: fighting the metabolic syndrome, *Cell Metab.* **13**, 238–240 (2011).

141. D. F. Vatner *et al.*, Thyroid hormone receptor- agonists prevent hepatic steatosis in fat-fed rats but impair insulin sensitivity via discrete pathways, *AJP Endocrinol. Metab.* **305**, E89–E100 (2013).

142. J. Z. Lin *et al.*, Thyroid hormone receptor agonists reduce serum cholesterol independent of the LDL receptor, *Endocrinology* **153**, 6136–6144 (2012).

143. M. López *et al.*, Hypothalamic AMPK and fatty acid metabolism mediate thyroid regulation of energy balance, *Nat. Med.* **16**, 1001–1008 (2010).

144. L. Ye *et al.*, Fat cells directly sense temperature to activate thermogenesis, *Proc. Natl. Acad. Sci. U. S. A.* **110**, 12480–12485 (2013).

145. J. E. Silva, Thermogenic mechanisms and their hormonal regulation, *Physiol. Rev.* **86**, 435–464 (2006).

146. U. Sundin, GDP binding to rat brown fat mitochondria: effects of thyroxine at different ambient temperatures, *Am. J. Physiol.* **241**, C134–139 (1981).

147. T. Sato, E. Imura, A. Murata, N. Igarashi, Thyroid hormone-catecholamine interrelationship during cold acclimation in rats. Compensatory role of catecholamine for altered thyroid states, *Acta Endocrinol. (Copenh.)* **113**, 536–542 (1986).

148. S. Rehnmark *et al.*, Brown adipocytes differentiated in vitro can express the gene for the uncoupling protein thermogenin: effects of hypothyroidism and norepinephrine, *Exp. Cell Res.* **182**, 75–83 (1989).

149. E. Yehuda-Shnaidman, B. Buehrer, J. Pi, N. Kumar, S. Collins, Acute stimulation of white adipocyte respiration by PKA-induced lipolysis, *Diabetes* **59**, 2474–2483 (2010).

150. Y. K. Luu *et al.*, In vivo quantification of subcutaneous and visceral adiposity by micro-computed tomography in a small animal model, *Med. Eng. Phys.* **31**, 34–41 (2009).

151. L. Calderan *et al.*, In vivo phenotyping of the ob/ob mouse by magnetic resonance imaging and 1H-magnetic resonance spectroscopy, *Obes. Silver Spring Md* **14**, 405–414 (2006).